NAVAL POSTGRADUATE SCHOOL
Monterey, California

THESIS

SMART ANTENNA IN DS-CDMA MOBILE COMMUNICATION SYSTEM USING CIRCULAR ARRAY TECHNIQUE

by

Stewart Siew Loon Ng

March 2003

Thesis Advisor:	Tri Ha
Co-Advisor:	Jovan Lebaric

Approved for public release, distribution is unlimited

THIS PAGE INTENTIONALLY LEFT BLANK

REPORT DOCUMENTATION PAGE			Form Approved OMB No. 0704-0188
Public reporting burden for this collection of information is estimated to average 1 hour per response, including the time for reviewing instruction, searching existing data sources, gathering and maintaining the data needed, and completing and reviewing the collection of information. Send comments regarding this burden estimate or any other aspect of this collection of information, including suggestions for reducing this burden, to Washington headquarters Services, Directorate for Information Operations and Reports, 1215 Jefferson Davis Highway, Suite 1204, Arlington, VA 22202-4302, and to the Office of Management and Budget, Paperwork Reduction Project (0704-0188) Washington DC 20503.			
1. AGENCY USE ONLY ***(Leave blank)***	**2. REPORT DATE** March 2003	**3. REPORT TYPE AND DATES COVERED** Master's Thesis	
4. TITLE AND SUBTITLE: Smart Antenna in DS-CDMA Mobile Communication System using Circular Array			**5. FUNDING NUMBERS**
6. AUTHOR(S) Stewart Siew Loon Ng			
7. PERFORMING ORGANIZATION NAME(S) AND ADDRESS(ES) Naval Postgraduate School Monterey, CA 93943-5000			**8. PERFORMING ORGANIZATION REPORT NUMBER**
9. SPONSORING /MONITORING AGENCY NAME(S) AND ADDRESS(ES) N/A			**10. SPONSORING/MONITORING AGENCY REPORT NUMBER**
11. SUPPLEMENTARY NOTES The views expressed in this thesis are those of the author and do not reflect the official policy or position of the Department of Defense or the U.S. Government.			
12a. DISTRIBUTION / AVAILABILITY STATEMENT Approved for public release, distribution is unlimited			**12b. DISTRIBUTION CODE**

13. ABSTRACT ***(maximum 200 words)***

This thesis examines a circular adaptive antenna array used at the mobile station for a typical Direct Sequence Code Division Multiple Access (DS-CDMA) cellular mobile communications system. The primary objective is to reduce co-channel interference of a wideband CDMA cellular network under a multi-path fading environment. We analyzed the performance of a randomly positioned mobile terminal with a randomly orientated adaptive antenna array in the forward channel (base-station to mobile) of a multi-cell DS-CDMA system and established four performance boundaries.

A single complex circular adaptive weight in each element channel of a circular adaptive array sufficiently processes narrowband signals. However, in order to process broadband signals, a tapped-delay line (transveral filter) is required. This tapped-delay line is employed because it can adjust the frequency dependent amplitude and phase. The performance of a DS-CDMA cellular system with a mobile terminal equipped with a circular array and a tapped-delay line is analyzed. It has been demonstrated that the optimization process has been extremely computationally expensive and hence minimum taps should be used for practical considerations. The results illustrated that, in general, for a four-element circular array system, a two tapped-delay line would be sufficient to equalize the broadband signal while providing a similar performance level to that of a narrow-band adaptive array system.

14. SUBJECT TERMS Smart Antenna, Uniform Circular Array, Hata Model, Rayleigh Fading, DS-CDMA, and Tapped-Delay Line			**15. NUMBER OF PAGES** 101
			16. PRICE CODE
17. SECURITY CLASSIFICATION OF REPORT Unclassified	**18. SECURITY CLASSIFICATION OF THIS PAGE** Unclassified	**19. SECURITY CLASSIFICATION OF ABSTRACT** Unclassified	**20. LIMITATION OF ABSTRACT** UL

NSN 7540-01-280-5500 Standard Form 298 (Rev. 2-89)
Prescribed by ANSI Std. 239-18

THIS PAGE INTENTIONALLY LEFT BLANK

Approved for public release, distribution is unlimited

SMART ANTENNA IN DS-CDMA MOBILE COMMUNICATION SYSTEM USING CIRCULAR ARRAY TECHNIQUE

Stewart Siew Loon Ng
Major, Republic of Singapore Air Force
Bachelor of Engineering (Hons), University of Leeds, UK, 1996
Master in International Business, University of Wollongong, Australia, 2000

Submitted in partial fulfillment of the
requirements for the degree of

MASTER OF SCIENCE IN ELECTRICAL ENGINEERING

from the

NAVAL POSTGRADUATE SCHOOL
March 2003

Author: Stewart Siew Loon Ng

Approved by: Tri. T Ha
Thesis Advisor

Jovan Lebaric
Co-Advisor

John P. Powers
Chairman, Department of Electrical and Computer Engineering

THIS PAGE INTENTIONALLY LEFT BLANK

ABSTRACT

This thesis examines a circular adaptive antenna array used at the mobile station for a typical Direct Sequence Code Division Multiple Access (DS-CDMA) cellular mobile communications system. The primary objective is to reduce co-channel interference of a wideband CDMA cellular network under a multi-path fading environment. We analyzed the performance of a randomly positioned mobile terminal with a randomly orientated adaptive antenna array in the forward channel (base-station to mobile) of a multi-cell DS-CDMA system and established four performance boundaries.

A single complex circular adaptive weight in each element channel of a circular adaptive array sufficiently processes narrowband signals. However, in order to process broadband signals, a tapped-delay line (transveral filter) is required. This tapped-delay line is employed because it can adjust the frequency dependent amplitude and phase. The performance of a DS-CDMA cellular system with a mobile terminal equipped with a circular array and a tapped-delay line is analyzed. It has been demonstrated that the optimization process has been extremely computationally expensive and hence minimum taps should be used for practical considerations. The results illustrated that, in general, for a four-element circular array system, a two tapped-delay line would be sufficient to equalize the broadband signal while providing a similar performance level to that of a narrowband adaptive array system.

THIS PAGE INTENTIONALLY LEFT BLANK

TABLE OF CONTENTS

I. INTRODUCTION....1

II. OVERVIEW OF SMART ANTENNA TECHNOLOGY....5

III. SMART ANTENNA APPLICATION IN MOBILE COMMUNICATIONS....13
- A. CO-CHANNEL INTERFERENCE....13
- B. SECTORING....15
- C. ADAPTIVE ANTENNA ARRAYS APPLICATION IN CDMA/TDMA FORWARD CHANNEL....17

IV. CIRCULAR ADAPTIVE ANTENNA ARRAY....21
- A. CHANNEL ILLUSTRATION....22
- B. WEIGHTING OPTIMIZATION....26
- C. CIRCULAR ARRAY CHARACTERISTICS....28
  - 1. Radiation Pattern....28
  - 2. Antenna Angular Spread and Spacing....30

V. PERFORMANCE ANALYSIS OF ADAPTIVE ANTENNA SYSTEM IN A CIRCULAR PATTERN....31
- A. PATH LOSS COMPONENTS....31
  - 1. Hata Model....31
  - 2. Log-normal Shadowing....33
  - 3. Multi-path Fading....34
- B. PERFORMANCE ANALYSIS FOR CIRCULAR ADAPTIVE ARRAY....36
- C. NAKAGAMI-M LOG-NORMAL CHANNEL FADING MODEL....52
- D. ADVANTAGES OF UCA OVER ULA....57
  - 1. 360° Field of View and Symmetry....57
  - 2. Antenna Separation....59
  - 3. UCA in Space-Time Adaptive Processing Application....61

VI. PERFORMANCE ANALYSIS OF WIDEBAND ADAPTIVE ANTENNA SYSTEM USING TAPPED-DELAY LINE....63

VII. CONCLUSIONS AND FUTURE WORK....73
- A. CONCLUSIONS....73
- B. FUTURE WORK....74
  - 1. Planar Adaptive Array....74
  - 2. Jamming....75
  - 3. Smart Antenna in 3/4G Technologies....75

LIST OF REFERENCES....77

INITIAL DISTRIBUTION LIST....79

THIS PAGE INTENTIONALLY LEFT BLANK

LIST OF FIGURES

Figure 1. Switch-Beam System Coverage Patterns 6
Figure 2. Adaptive Array Coverage: A Representative Depiction of a Main Lobe. Extending toward a User with a Null Directed toward a Co-channel Interferer 7
Figure 3. Block Diagram of an Adaptive Antenna System (From Ref. [1].) 8
Figure 4. Laptop-mounted Dual-polarized Array Elements Spaced Half Wavelength Apart (From Ref. [4]) 10
Figure 5. Base Station Rooftop Antenna Array Used Dual-polarized Antennas (From Ref. [4]) 10
Figure 6. Geometry of a Cellular CDMA Mobile Communication Network 15
Figure 7. 60° and 120° Cell Sectoring 16
Figure 8. Probability of Bit Error for DS-CDMA Using Sectoring ($\sigma_{\mathrm{dB}} = 7$) with an SNR per bit of 15 dB with Rate 1/2 Convolution Encoder with $\nu = 8$ (From Ref. [3]) 17
Figure 9. Common Antenna Array Geometries — Uniform Linear Array ULA (Left) and Uniform Circular Array UCA (right) 22
Figure 10. Uniform Circular Array Geometry 23
Figure 11. Block Diagram of an Adaptive Antenna System (From Ref. [1].) 25
Figure 12. Radiation Pattern of a Four-Antenna Circular Antenna Array. 29
Figure 13. Multi-path Effects 35
Figure 14. Types of Small-Scale Fading (From Ref. [2]) 36
Figure 15. Radiation Pattern for a Three-Element Circular Array with 2 Interferers 39
Figure 16. Radiation Pattern for a Four-Element Circular Array with 2 Interferers 39
Figure 17. Radiation Pattern for a Four-Element Circular Array with 3 Interferers 40
Figure 18. Radiation Pattern for a Five-Element Circular Array with 4 Interferers 40
Figure 19. Radiation Pattern for a Six-Element Circular Array with 4 Interferers 41
Figure 20. Performance for the DS-CDMA System with a Three-Element ULA ($\sigma_{\mathrm{dB}} = 7$) for $N = 128$ in a Rayleigh Fading Channel 45
Figure 21. Performance for the DS-CDMA System with a Three-Element UCA ($\sigma_{\mathrm{dB}} = 7$) for $N = 128$ in a Rayleigh Fading Channel 45
Figure 22. Performance for the DS-CDMA System with a Three-Element ULA ($\sigma_{\mathrm{dB}} = 8$) for $N = 128$ in a Rayleigh Fading Channel 46
Figure 23. Performance for the DS-CDMA System with a Three-Element UCA ($\sigma_{\mathrm{dB}} = 8$) for $N = 128$ in a Rayleigh Fading Channel 46
Figure 24. Performance for the DS-CDMA System with a Three-Element ULA ($\sigma_{\mathrm{dB}} = 9$) for $N = 128$ in a Rayleigh Fading Channel 47
Figure 25. Performance for the DS-CDMA System with a Three-Element UCA ($\sigma_{\mathrm{dB}} = 9$) for $N = 128$ in a Rayleigh Fading Channel 47

Figure 26. Performance for the DS-CDMA System with a Four-Element ULA (σ_{dB} = 7) for $N = 128$ in a Rayleigh Fading Channel 49
Figure 27. Performance for the DS-CDMA System with a Four-Element UCA (σ_{dB} = 7) for $N = 128$ in a Rayleigh Fading Channel 49
Figure 28. Performance for the DS-CDMA System with a Four-Element ULA (σ_{dB} = 8) for $N = 128$ in a Rayleigh Fading Channel 50
Figure 29. Performance for the DS-CDMA System with a Four-Element UCA (σ_{dB} = 8) for $N = 128$ in a Rayleigh Fading Channel 50
Figure 30. Performance for the DS-CDMA System with a Four-Element ULA (σ_{dB} = 9) for $N = 128$ in a Rayleigh Fading Channel 51
Figure 31. Performance for the DS-CDMA System with a Four-Element UCA (σ_{dB} = 9) for $N = 128$ in a Rayleigh Fading Channel 51
Figure 32. Performance for the DS-CDMA System with a Four-Element UCA (σ_{dB} = 7) for a Nakagami-m Log-normal Channel Fading Model with $m = 3$ 54
Figure 33. Performance for the DS-CDMA System with a Four-Element UCA (σ_{dB} = 7) for a Nakagami-m Log-normal Channel Fading Model with $m = 5$ 54
Figure 34. Performance for the DS-CDMA System with a Four-Element UCA (σ_{dB} = 8) for a Nakagami-m Log-normal Channel Fading Model with $m = 3$ 55
Figure 35. Performance for the DS-CDMA System with a Four-Element UCA (σ_{dB} = 8) for a Nakagami-m Log-normal Channel Fading Model with $m = 5$ 55
Figure 36. Performance for the DS-CDMA System with a Four-Element UCA (σ_{dB} = 9) for a Nakagami-m Log-normal Channel Fading Model with $m = 3$ 56
Figure 37. Performance for the DS-CDMA System with a Four-Element UCA (σ_{dB} = 9) for a Nakagami-m Log-normal Channel Fading Model with $m = 5$ 56
Figure 38. A Three-Element ULA with an Interfering Signal Directly Opposite the Desired Signal (From Ref. [5].) 58
Figure 39. A Three-Element UCA with an Interfering Signal Directly Opposite the Desired Signal 58
Figure 40. A Three-Element Linear Array Antenna Factor with ISR = –7.12 dB and $d = \lambda/2$ (From Ref. [5].) 59
Figure 41. A Three-Element Linear Array Antenna Factor with ISR = –127.84 dB and $d = \lambda$ (From Ref. [5].) 60
Figure 42. 8-element UCA 60
Figure 43. Wideband *K*-Element Array with an *L*-Tapped-Delay Line 64
Figure 44. Desired Signal (SBS) and Interference Signal (IBS) Transfer Functions of a Three Element Array with a Two Tapped-Delay Line System and 4% Bandwidth 67
Figure 45. Desired Signal (SBS) and Interference Signal (IBS) Transfer Functions of a Three Element Array with a Three Tapped-Delay Line System and 4% Bandwidth 67
Figure 46. Desired Signal (SBS) and Interference Signal (IBS) Transfer Functions of a Three Element Array with a Five Tapped-Delay Line System and 4% Bandwidth 68

Figure 47. Desired Signal (SBS) and Interference Signal (IBS) Transfer Functions of a Four Element Array with a Two Tapped-Delay Line System and 4% Bandwidth 69
Figure 48. Desired Signal (SBS) and Interference Signal (IBS) Transfer Functions of a Four Element Array with a Three Tapped-Delay Line System and 4% Bandwidth 69
Figure 49. Desired Signal (SBS) and Interference Signal (IBS) Transfer Functions of a Four Element Array with a Five Tapped-Delay Line System and 4% Bandwidth 70

THIS PAGE INTENTIONALLY LEFT BLANK

LIST OF TABLES

Table 1. Simulation Results Using UCA with a Different Number of Elements and the Associated Interferers 42

THIS PAGE INTENTIONALLY LEFT BLANK

ACKNOWLEDGMENTS

This thesis is dedicated to my family, especially my loving wife, Krisline, my beautiful daughter, Alicia, and my adorable son, Amos, for enduring my stress and absence during my research here at the Naval Postgraduate School. I am forever indebted to them for their love, consideration, and unrelenting support that continually inspired me to visualize reality from a different perspective.

I also wish to dedicate this thesis to my thoughtful and supportive parents who taught me the values of education, diligence and conscientiousness.

I would like to express my sincere appreciation to my advisors, Professor Tri. Ha and Professor Jovan Lebaric. Without their support coupled with clear explanations and supervision, this thesis would not have been possible.

Lastly, I must thank my sponsor, the Republic of Singapore Air Force, for providing an opportunity for me to pursue my postgraduate study here in the Naval Postgraduate School.

THIS PAGE INTENTIONALLY LEFT BLANK

EXECUTIVE SUMMARY

Wireless communications for mobile telephone and data transmission face ever-changing demands on their spectrum and infrastructure resources. Increased minutes of use, capacity-intensive data applications, and the steady growth of worldwide wireless subscribers mean carriers must effectively accommodate increased wireless traffic in their networks. However, deploying new cell sites is not the most economical or efficient means of increasing capacity. Wireless carriers have begun to explore new ways to maximize the spectral efficiency of their networks and to improve their return on investment. Smart antennas have emerged as one of the leading innovations for achieving highly efficient networks that maximize capacity and improve quality and coverage.

The early smart antennas were designed for governmental use in military applications, which used directed beams to hide transmissions from an enemy. This thesis will also present the application of the smart antenna technology at the mobile terminal, for the third-generation DS-CDMA cellular system can be extended to the military mobile communication systems. Smart antennas have the following advantages in military wireless systems:

- Increase coverage
- Increase communication quality
- Increase capacity
- Lower handset power consumption
- Indicate user location by direction finding
- Reduce interference to other users

Related techniques for clutter cancellation in a radar system can be achieved with smart-antenna like space-time adaptive processing. Smart antennas are considered to be the last major technological innovation that can potentially and vastly increase a wireless-communication system's performance.

The emerging third-generation (3G) cellular system that employs Direct Sequence Code Division Multiple Access (DS-CDMA) will incorporate considerable signal processing intelligence in order to provide advanced services, such as multimedia transmission, allowing simultaneous sharing of limited available bandwidth. In fact, 3G services are already a reality for many users in Japan, Korea and in Europe. However, two major factors limit the performance of DS-CDMA systems: multiple access interference and multi-path channel distortion. Many advanced signal-processing techniques have been proposed to combat these factors. Among these techniques, one of the more promising is using a Smart or Adaptive antenna array. A smart antenna system combines an antenna array with a digital signal-processing capability to transmit and to receive in an adaptive, spatially sensitive manner. In other words, such a system can change the directionality of its radiation patterns in response to its signal environment. This can dramatically increase the performance characteristics, such as the capacity of a wireless system.

This thesis analyzes the performance of the base-station to the mobile channel (forward channel) of a DS-CDMA system in a slow, flat Rayleigh fading and Nakagami-m log-normal shadowing environment. The forward channel is being studied because the majority of the data services are asymmetric, with the downstream entailing a higher data rate more frequently. We explore the use of an adaptive circular-array antenna at the mobile terminal in order to suppress the interferers. This is achieved by precisely controlling the signal nulls quality toward the interferers and by mitigating interference while forming an antenna beam toward the desired signal continuously with time.

As such, with a certain adaptive technologies that can support the reusing of frequencies within the same cell coupled with minimizing the interference-to-signal ratio will drastically improve the system's performance and overall capacity. In addition, four performance boundaries of the DS-CDMA mobile communication system with an adaptive array were established. The worst-case performance of the system was compared with a DS-CDMA system without the smart antenna application and also with a smart antenna arranged in a linear pattern.

The thesis further explores the simulation strategy that evaluates the improvement in the performance of various receiving antenna by using a wideband smart antenna

(Tapped-Delay Line) system. In the case of a four-element circular array, we demonstrate that a two tapped-delay lines sufficiently equalize and compensate for the frequency variation of a 4% bandwidth broadband signal.

THIS PAGE INTENTIONALLY LEFT BLANK

I. INTRODUCTION

Extensive research on smart antenna cellular applications started in the early 1990's. Interest in this technology has steadily increased since spatial processing is considered as a "last frontier" in the battle for cellular system capacity with a limited amount of the radio spectrum. Network performance is a complex subject that includes network capacity, call quality, data throughput and other parameters that directly impact the performance seen by the customer. In wireless networks, performance is limited by radio frequency (RF) interference. There is a trade-off between the number of users communicating on the network and the performance that they will experience; having more subscribers results in higher RF interference and lower performance quality. As such, reducing network-wide interference has become critical. The smart antenna techniques are one of the few techniques that are currently proposed for new cellular radio network designs. These will be able to improve the system's performance dramatically.

There is a trend to adopt commercial off-the-shelf products for military applications, as this approach may be more cost effective. With slight modification of the commercial mobile communication system, the modified system can be deployed for military applications. Hence, the performance analysis in the application of the smart antenna technology at the mobile terminal for the third-generation DS-CDMA cellular system that was presented in this thesis should be worthy for military use.

In general, the most complex and expensive part of the radio for these systems is the base station. As a result, manufacturers have been designing networks with high efficiency in terms of bandwidth occupied and the number of users per base station. This trend has been at the expense of high power transmitters and receivers, which employ very computationally expensive signal processing techniques. Nonetheless, this thesis investigates the performance of the forward channel (base-station to mobile) of a DS-CDMA system in a slow, flat Rayleigh fading and Nakagami-m lognormal shadowing environment. Generally, data services are asymmetric, with the downstream demanding a much high data rate. The forward channel is used to download data from sources, such as the Internet download, at a high data rate from the base-station to the mobile terminal.

The second generation of cellular telephones based on digital signaling and time and frequency division multiple access have been widely used throughout the world for many years. Typical examples include the European Global System for Mobile Telecommunications (GSM) and the North American IS-54 access protocol. The IS-95 standard for Code Division Multiple Access (CDMA) cellular systems was published in 1992; there is also significant interest in CDMA systems for the US for the 1.9 GHz PCS bands and the European third-generation universal mobile telephone system (UMTS). The third-generation (3G) cellular system employs a multiple-access technique known as Direct Sequence Code Division Multiple Access (DS-CDMA). This technique is based on spread-spectrum communications, which were originally developed for military applications. A simple definition of a spread-spectrum signal is that its transmission bandwidth is much wider than the bandwidth of the original signal. Simultaneous multiple-user access in such a system efficiently exploits the limited bandwidth. However, the DS-CDMA scheme used in the cellular system also creates network problems, such as inter-cell co-channel interference and intra-cell interference.

As wireless networks mature and the rate of subscribers plateaus, the focus on customer retention and satisfaction becomes increasingly important. This occurs at a time when the widespread use of mobile communications has heightened consumer demand for quality service anytime or anywhere. Network operators face the challenges of improving the quality of service while increasing capacity and adding contemporary data services. These challenges are also true for operators of less mature networks seeking to differentiate their brands and services. Hence, network performance plays an increasing role in affecting the operator's bottom line.

Optimum combining techniques have traditionally been used to combine the different antenna branches in antenna arrays to create nulls toward interfering signals while maintaining large antenna gain toward the desired signal. Optimum combining requires that an optimum complex weight must be found for each antenna signal. These weights form a weight vector $\boldsymbol{W}$, which can be optimized using different algorithms and criteria. For example, minimum-mean-squared-error (MMSE), maximum signal-to-interference-plus-noise ratio (SINR), maximum likelihood (ML) and minimum noise variance (MV) criteria can be applied. All the criteria lead to a similar weight vector, which is propor-

tional to the signal strengths of the desired and undesired signals and their covariance. A mobile communication system often encounters co-channel interferers who occupy the same channel as the desired user and thus limit the system's performance and capacity. The most modern method of using dual diversity with Maximum Ratio Combining at the receiver cannot reduce the high interference. This is because the strategy of selecting the strongest signal or extracting the maximum signal power from the antennas is not appropriate. This method will enhance the interferer signal rather than the desired signal. Nonetheless, if we could estimate the direction of arrival (DoA) of the interferers and the desired signal, we could then use an adaptive antenna array to suppress the interference by steering a null toward the interferer and forming a beam toward the desired signal continuously with time. Consequently, the dynamic system performance can be improved significantly.

In this thesis, we implemented a circular antenna array with at least three elements at the mobile terminal. We analyzed the performance of a randomly positioned mobile terminal with a randomly oriented adaptive antenna array in a multi-cell DS-CDMA network and established four performance boundaries. We selected the tighter optimized array antenna boundary as our performance reference, as it is more conservative and represents the worst-case situation. We then combined the conservative optimized circular element array antenna with the DS-CDMA forward-channel received signal model developed in Ref. [3]. The model in Ref. [3], which originally incorporated both log-normal shadowing and Rayleigh slow-flat fading, now included the effect of the smart antenna. Ultimately, we compared the capacity and performance of different cellular systems under a range of shadowing conditions, with and without antenna sectoring at the base-station and for various user capacities.

All the previous analyses assumed that the system is a narrowband system. A single complex circular adaptive weight in each element channel of a circular adaptive array sufficiently processes narrowband signals. However, in order to process broadband signals, a tapped-delay line (transveral filter) is required. This tapped-delay line was employed because it could adjust the frequency dependent amplitude and phase. In a practical implementation, each channel is slightly different electrically and will lead to channel mismatching, which could significantly alter the frequency response characteristics from

channel to channel. This may severely degrade the antenna array performance. The tapped-delay line permits frequency-dependent amplitude and phase adjustments to be made, to equalize the frequency-varying effect on the antenna when receiving a broad-band signal. The performance of a DS-CDMA cellular system with a mobile terminal equipped with a circular array and a tapped-delay line is analyzed. It has been demonstrated that the optimization process has been extremely computationally expensive and hence minimum taps should be used for practical considerations. The results show that, in general, for a four-element circular array system, a two tapped-delay lines sufficiently equalize and compensate for the frequency variation of a 4% bandwidth broadband signal.

The thesis is organized as follows: Chapter II presents an overview and historical background of smart antenna technology. Chapter III reviews the co-channel interference of a DS-CDMA system and various methods to minimize the interference problem. Chapter IV introduces the characteristics and constraints of a circular adaptive array system using a DS-CDMA system for the analysis. Chapters V and VI discuss the performance of an adaptive antenna system in a narrow-band and a wide-band DS-CDMA forward channel respectively. Chapter VII presents a summary and proposes prospective developmental work in this arena.

II. OVERVIEW OF SMART ANTENNA TECHNOLOGY

The technology of smart or adaptive antennas for mobile communications has received enormous worldwide interest recently. This chapter examines the technology and the different ways in which it will likely influence mobile communications systems. The principal reason for introducing smart antennas is that they can potentially increase capacity: an increase of three times for Time-Division Multiple Access (TDMA) systems and five times for Code-Division Multiple Access (CDMA) systems have been reported [4]. Other advantages include increased range and the potential to introduce new services. It is foreseen that in the near future an enormous increase in traffic will be experienced for mobile and personal communications systems. This is due both to an increased number of users as well as to the introduction of new high bit rate data services. This trend is observed for second-generation systems and will most certainly continue for third-generation systems introduced worldwide within the next few years. The increase in traffic has placed a demand on both manufacturers and operators to provide enough capacity in the networks. Presently, one of the most promising techniques for increasing the capacity in cellular systems is a smart or adaptive antenna.

The theory behind smart antennas is not new. For many years, this technique has been used in electronic warfare (EWF) as a countermeasure for electronic jamming. In military radar systems similar techniques were even used during World War II. An adaptively adjustable antenna beam can be generated in a number of ways, for instance, by mechanically steering the antennas. However, the technology exclusively suggested for land-based mobile and personal communications systems is accomplished by using array antennas. The main philosophy is that interferers rarely have the same geographical location as the user. Maximizing the antenna gain in the desired direction and simultaneously placing a minimal radiation pattern in the directions of the interferers can significantly improve the quality of the communication link. In personal and mobile communications, the interferers are users other than the user being addressed.

Smart antennas are classified into two main types: Switched Beam and Adaptive Array. A switched-beam antenna system forms multiple fixed beams with heightened sensitivity in particular directions as shown in Figure 1. These antenna systems detect signal strength, choose from one of the several predetermined fixed beams, and then switch from one beam to another as the mobile moves throughout the sector. In addition, the antenna system also measures the RF power or signal strength from a set of pre-defined beams and outputs the RF from the selected beams that afford the best performance to a desired user.

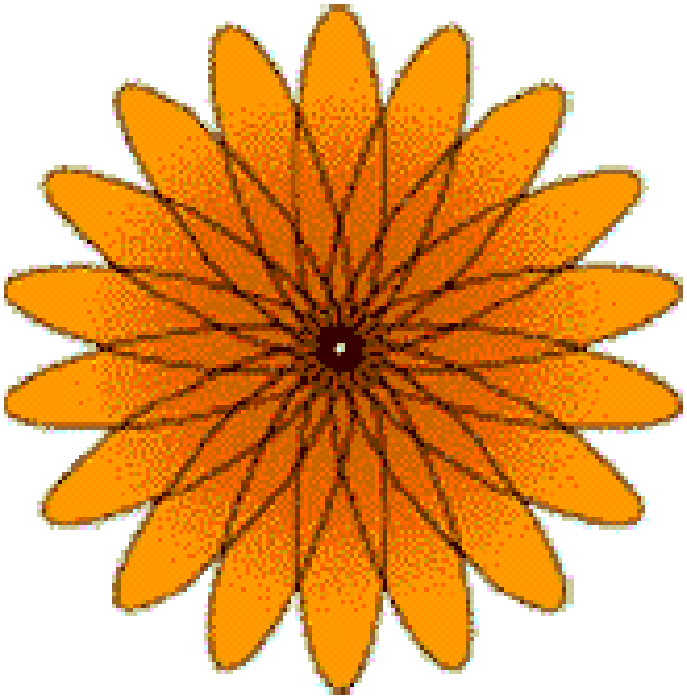

Figure 1. Switch-Beam System Coverage Patterns

Adaptive antenna technology represents the most advanced smart antenna approach to date. Antenna arrays when used in an appropriate configuration, at the base station, in mobile communications significantly improve the system's performance by increasing channel capacity and spectrum efficiency. Arrays can also help reduce multi-path fading thus increasing coverage. Most smart antennas form beams that are directed to a particular user in order to enhance the received signal strength and signal-to-noise ratio (SNR) as shown in Figure 2. The signals are first down-converted to an intermedi-

ate frequency (IF), then digitized, weighted and summed in a pre-defined processing algorithm. In general, all smart antennas direct their main beam with an increased gain, in the direction of the user (they may guide nulls in the direction of the interfering signal as well). Although both switched beam and adaptive array systems have this in common, only the adaptive array system offers optimal gain, while simultaneously identifying, tracking, and minimizing reception of interfering signals. The system's null forming capability offers substantial performance advantages over the more passive switched beam approach by enabling the maximum interference suppression.

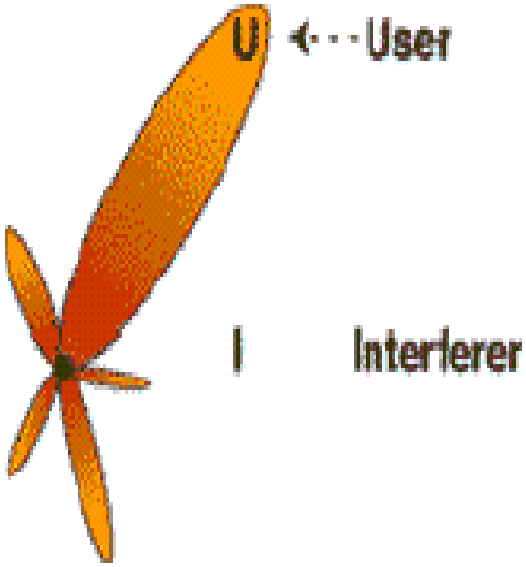

Figure 2. Adaptive Array Coverage: A Representative Depiction of a Main Lobe. Extending toward a User with a Null Directed toward a Co-channel Interferer

Adaptive arrays are further classified into two types: dynamic phased arrays and adaptive antenna arrays. Dynamic phased arrays use the direction of arrival (DoA) information from the desired user and steer a beam maximum toward the desired user. This allows continuous tracking of the user, thus improving the capabilities of a switched - beam antenna. In an adaptive antenna array, the weights are adjusted to maximize the signal-to-interference-plus-noise ratio (SINR) and provide the maximum discrimination against interfering signals. In the absence of interferers and with noise as the only unde-

sired signal, adaptive antennas maximize the signal-to-noise ratio (SNR) and thus perform as a maximum ratio combiner (MRC). By using a variety of signal processing algorithms, the adaptive antenna system can continuously distinguish between the desired signal and the interfering signal and can maximize the intended signal reception. As shown in Figure 3, an adaptive antenna array system, a DoA for determining the direction of interfering sources is introduced and the adaptive antenna array will steer null patterns toward these interferers. In addition, by using special algorithms and branch diversity techniques, the adaptive antenna array can process and resolve separate multi-path signals, which can later be combined. This technique can maximize the signal-to-interference and noise ratio (SINR). Adaptive antenna arrays with *N* antennas can be regarded as an *N*-branch diversity scheme, providing more than the traditional two diversity branches.

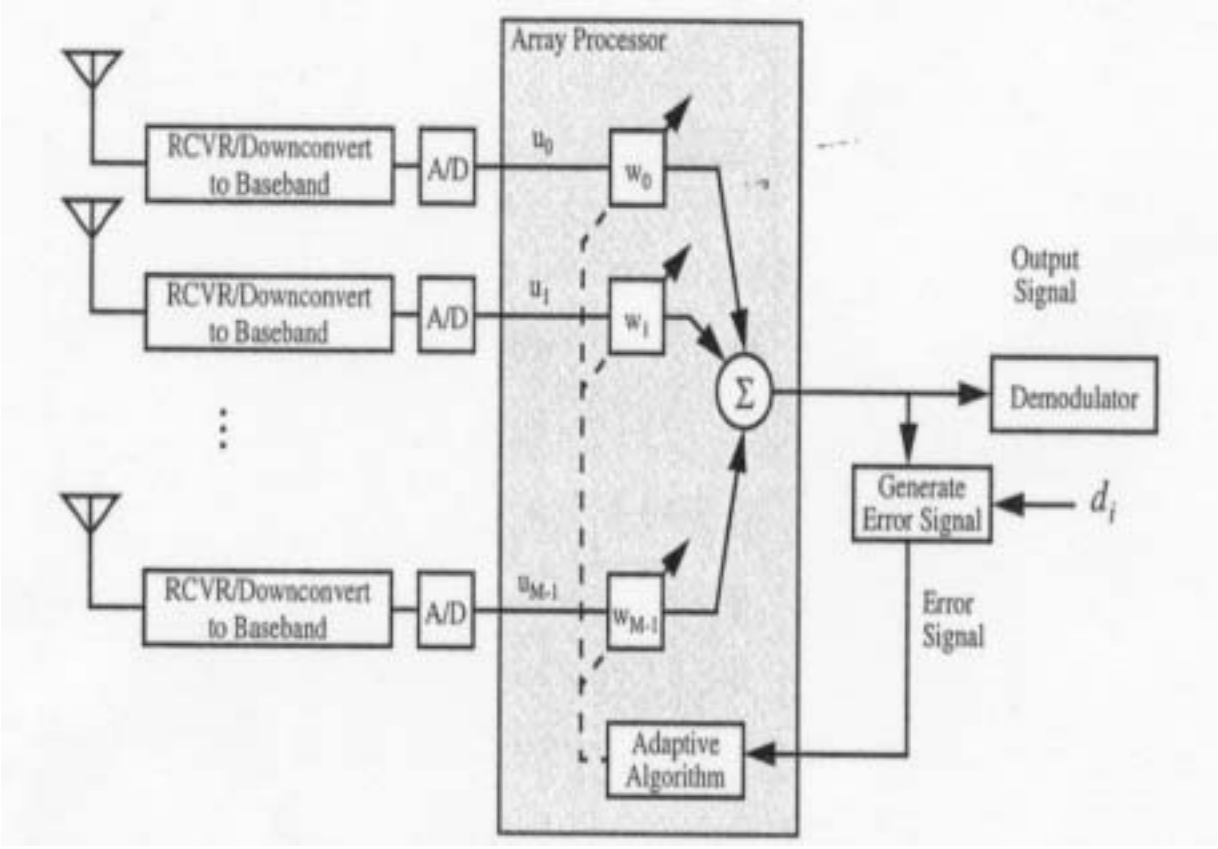

Figure 3. Block Diagram of an Adaptive Antenna System (From Ref. [1].)

The RF signals from the *N* antenna elements are coherently down-converted to an IF frequency, low enough for quality digitization of the signals. The beamformer then processes the digital outputs for each channel by adjusting the amplitude and phase of the signals by further adjusting the weights with which the signal will be multiplied. This will result in beam and null steering. The adaptive antenna system can be viewed as a spatial filter in which the pass and stop band is created along the direction of the signal and interferers respectively.

3G systems have been designed to provide relatively high-rate data services. However, these systems are still limited by the quality of over-the-air communication channels just as 2G systems are; the Shannon limit is a fundamental limit. Standards bodies have recognized the value of smart antennas in improving signal-to-noise ratios and have made provisions for such systems in the emerging 3G standards. For example, Wideband Code-Division Multiple Access (WCDMA) and CDMA2000 allow dedicated pilot channels for each mobile user on both the forward and reverse links. In order to realize the benefits of such dedicated or auxiliary pilots, smart antenna systems are required. As a result, smart antennas are regarded as one of the essential components in the 3G systems.

Presently, many systems are undergoing research and trial. Figure 4 shows a four-branch transmitter mobile system with antennas mounted on a laptop computer and Figure 5 shows a base station rooftop antenna array used dual-polarized antennas.

Figure 4. Laptop-mounted Dual-polarized Array Elements Spaced Half Wavelength Apart (From Ref. [4])

Figure 5. Base Station Rooftop Antenna Array Used Dual-polarized Antennas (From Ref. [4])

Smart antenna systems improve the signal-to-noise figures in mobile communications networks and hence improve the quality of service. The high data rates and complex operating characteristics of 3G networks will require the precise and flexible interference control that smart antennas can provide. A soaring customer base is seriously exhausting the capacity of networks; even before data traffic becomes a significant source of traffic in most of the networks. As such, the most cost-effective solution to the current capacity limitations is the smart antenna systems.

This Chapter examined the technology and the different ways in which it will likely influence mobile communications systems. The next Chapter will discuss main constraint of a DS-CDMA mobile communication system and various methods to improve the system's capacity and performance.

THIS PAGE INTENTIONALLY LEFT BLANK

III. SMART ANTENNA APPLICATION IN MOBILE COMMUNICATIONS

This chapter presents the main constraint of a DS-CDMA mobile communication system and various methods to improve the system's capacity and performance. In cellular radio systems, the limited available bandwidth is one of the principal design constraints. The main constraint of the DS-CDMA network is the co-channel interference. Applying cell sectoring and smart antenna are methods commonly used to combat the co-channel interference.

A. CO-CHANNEL INTERFERENCE

Co-channel interference is a well-known and significant limitation in cellular and PCS wireless telephone networks. The generic model involves a hexagonally arranged circular cellular geometry, with each cell having six adjacent cells. A single base station is located in the center of each cell and any number of mobile stations is randomly located within a cell's radius. The interference model consists of two basic components as follows:

- Base-to-mobile link: Victim mobile stations are interfered by base stations in adjacent cells.
- Mobile-to-base link: Victim base station is interfered by mobile stations in adjacent cells

In the case of TDMA networks, the co-channel interference is mainly caused by the spectrum allocated for the system being reused multiple times. The problem may be more or less severe, depending on the reuse factor, but in all cases, a signal received by a handset will contain not only the desired forward channel from the current cell, but also signals originating in more distant cells. The possibility to reuse the same channels, the frequency bandwidth, in different cells is limited by the amount of co-channel interference between the cells. The minimum allowable distance between the nearby co-channel

cells or the maximum system capacity is based on the maximum tolerable co-channel interference at the receivers in the system.

In a multi-cell cluster, such as a TDMA IS-54/GSM system, interference can be suppressed by increasing the physical separation of co-channel cells until a sufficient isolation is achieved due to the propagation loss. Receivers resistant to co-channel interference allow a dense geographical reuse of the spectrum and thus a high system capacity. This can be achieved by increasing the cluster size *N*. The signal-to-interference (SIR) ratio, as defined in Ref. [2] is,

$$SIR = \frac{\left(\sqrt{3N}\right)^n}{i_o} \tag{3.1}$$

where n is the path loss exponent and i_o is the number of interferers.

CDMA technology provides enhanced capacity and signal qualities. In CDMA networks, all users access the same radio spectrum, but the system encodes and decodes individual signals from the total wide-band signal through uniquely assigned user codes As such, the multi-path signal fading environment and the multiple co-channel interferers limits the system's performance. With the co-channel interference as the major limiting factor for performance [2], the CDMA based network is hence an interference-limited system. Consequently in order to improve the system's performance and capacity, minimizing the system interference would be most effective. However, unlike thermal noise, which can be overcome by increasing the signal power, co-channel interference cannot be overcome by increasing the signal power as this will increase interference to the neighboring co-channel cells.

The whole frequency spectrum is shared and reused by all first-tier neighboring cells, the distance between the base-station to any co-channel base-station is fixed at $\sqrt{3}\,R$ where R is the radius of the hexagonal cell, as shown in Figure 6. Thus in the single-cell CDMA network, we do not have the freedom to vary the cluster size N to reduce the co-channel interference.

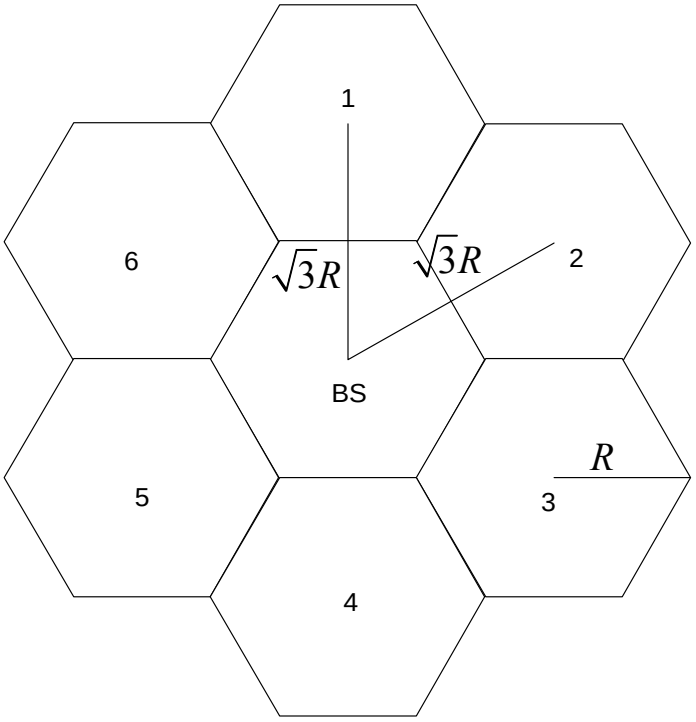

Figure 6. Geometry of a Cellular CDMA Mobile Communication Network

As a result, other methods should be explored in order to reduce the co-channel interference. The common methods to combat the co-channel interference — thus improving the system's performance —are by sectoring and by using smart antenna technology.

B. SECTORING

In TDMA systems, sectoring is done to reduce the co-channel interference. The trunking efficiency of these systems decreases due to sectoring and thus reduces the capacity. On the other hand, sectoring increases the capacity of CDMA systems. Sectoring is simply done by introducing three similar antennas in three sectors and the reduction in mutual interference due to this arrangement translates into a three-fold increase in capacity. In general, any isolation using multi-beamed or multi-sectored antennas provides an increase in the CDMA capacity. The isolation of the users in a CDMA system translates directly into an increase in the system's capacity. Consider an example in which three directional antennas having 120^0 effective beam-widths are employed. The interference

sources detected by any of these antennas are approximately one-third of those detected by the omni-directional antenna.

Replacing the omni-directional antenna at the base-station with several directional antennas can reduce the co-channel interference in a cellular mobile communication system. The use of a directional antenna limits the number of co-channel interferers detected by any receiver within the cell as each directional antenna only radiates within a desired sector. The scale of the reduction of the co-channel interference depends on the number of sectors used.

A cell is commonly partitioned into three 120^0 or six 60^0 sectors, as shown in Figure 7. In the case with the users evenly distributed within all cells, the amount of co-channel interference is reduced to 1/3 or 1/6 of the omni-directional value if 120^0 or 60^0 sectoring is used, respectively.

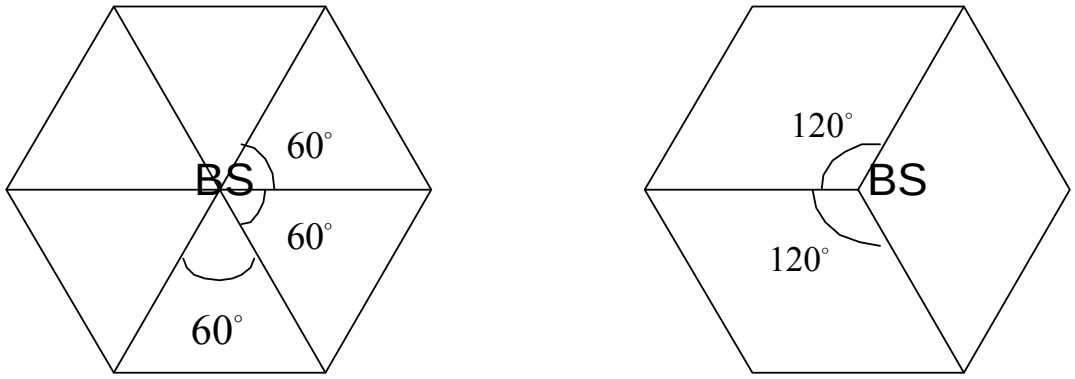

Figure 7. 60° and 120° Cell Sectoring

Many papers, such as Ref. [3], which evaluated the forward channel performance in the fading environment, evaluate and present the improved performance by using 6 and 3 sectors of 60^0 and 120^0, respectively, in a DS-CDMA cellular system operating in a channel with Rayleigh fading and log-normal shadowing as shown in Figure 8. It is clear that sectoring reduces interference, which amounts to an increase in capacity. For example, if the BER is fixed to be 10^{-3}, the number of users that the cell can accommodate is 10 for no sectoring and 40 when 120^0 sectoring is deployed.

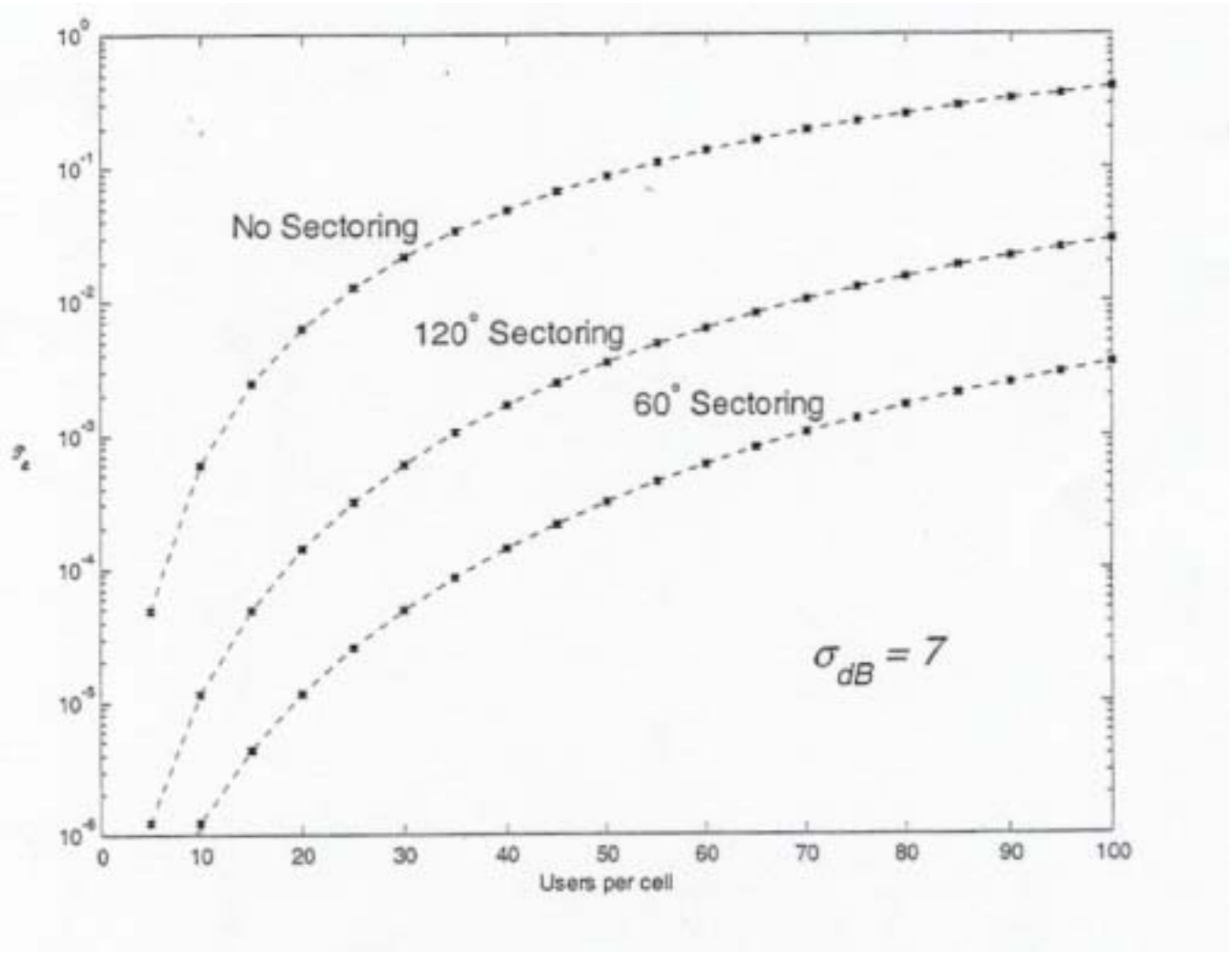

Figure 8. Probability of Bit Error for DS-CDMA Using Sectoring ($\sigma_{\text{dB}} = 7$) with an SNR per bit of 15 dB with Rate 1/2 Convolution Encoder with $v = 8$ (From Ref. [3])

C. ADAPTIVE ANTENNA ARRAYS APPLICATION IN CDMA/TDMA FORWARD CHANNEL

A principal difference between CDMA and other cellular standards makes it impossible to implement the same type, or equivalent, solution for smart antennas for CDMA as the solution implemented in TDMA (IS-54) standards. In TDMA systems, each user occupies a narrow bandwidth of 30 kHz within a given cellular bandwidth whenever the user is active. This makes it easy for the smart antenna to distinguish the

particular user's signal from the other users' signals (interferers) by simply filtering out the frequency of the user.

In GSM systems, several users may occupy the same RF channel, but they transmit their signal in bursts, so they are distinguished by different time slots within a RF channel. A base station controls the time slots synchronization and their time alignment. Therefore, GSM Smart antenna systems can isolate a particular user by filtering out the RF channel being used within the cellular bandwidth and synchronizing its receive gating circuitry with the mobile transmit bursts. Both smart antenna systems for these technologies take advantage of the discretization of the RF signal in frequency and time to preprocess the signal on the RF level before it arrives at a base station.

In CDMA systems, however, the users are distinguished by their assigned Walsh (forward channel) or PN (reverse channel) codes. In other words, all active users occupy all cellular bandwidth all the time, so there is no discretization in frequency or time. To identify a particular user, the CDMA system demodulates the Walsh or PN codes inside its radio, in base-band, after converting the received signal from RF to digital. Therefore, in order to track users in this system, the smart antenna must obtain information about the users from the CDMA radio, or it must be able to demodulate the RF signal on its own. Either of these is a very complex process or harder to implement than tracking the users previously described for other non-CDMA standards. Clearly, the only true "smart" solution that would track the user and null out interferers is by changing its pattern in real time.

Unlike the base-station, where the physical space is less of a constraint than on the laptop, implementing a larger number of antenna elements with a large signal processor is possible. However the mobile units do not have the luxury of the physical space of the base-station. In today's design of a mobile unit, reducing the physical size and weight is always a prime consideration. Implementing a large number of antenna elements on the mobile unit is not possible.

In this thesis, the performance of a three-element to seven-element adaptive circular-array system at the mobile user in the forward channel is analyzed because they fit into a mobile terminal in future communication systems.

This Chapter illustrated the requirement to combat the co-channel interference of a DS-CDMA mobile communication system. With the application of the smart antenna, the SINR of the system could be maximized. The next Chapter will discuss the characteristics and constraints of a circular-adaptive array for mobile communications.

THIS PAGE INTENTIONALLY LEFT BLANK

IV CIRCULAR ADAPTIVE ANTENNA ARRAY

As described in the last Chapter, a smart antenna system, such as an adaptive antenna array, can be applied to a CDMA mobile communication system to maximize the SINR of the system. The primary aim of the antenna array receiver is to provide acceptable error performance and to maximize the signal-to-interference and noise ratio (SINR) for each user in the system. An antenna array consists of N identical antenna receivers, whose operation and one central processor usually controls timing. The geometry of the antenna locations can vary widely, but the most common configurations are to place antennas in a circle (circular array), along a line (linear array) or in plane (planar array). The circular array geometry provides complete coverage from the base station as the beam can be steered through 360^0. As such, the position and spacing between antenna elements are very critical in the design of antenna arrays.

An antenna array containing N elements can provide a power gain of N over the white noise level, but suppressing interference from other users depends on the form of the received data. The adaptive antenna array steers a directional beam to maximize the signal from the desired user while nullifying the signals from the directions of interferers. It is possible to use the same physical antenna elements for all channels to adapt an independent beam pattern for each channel in the system. The antenna array consists of a number of antenna elements, which make it possible to radiate or to receive electromagnetic waves more effectively in some directions than in others. The radiated power distribution of an antenna array can be shown by a radiation pattern. The antenna array can take different geometries, and two common antenna arrays are the uniform linear array (ULA) and the uniform circular array (UCA) (see Figure 9.) This chapter presents the essential principles of UCA and compares the UCA and ULA systems.

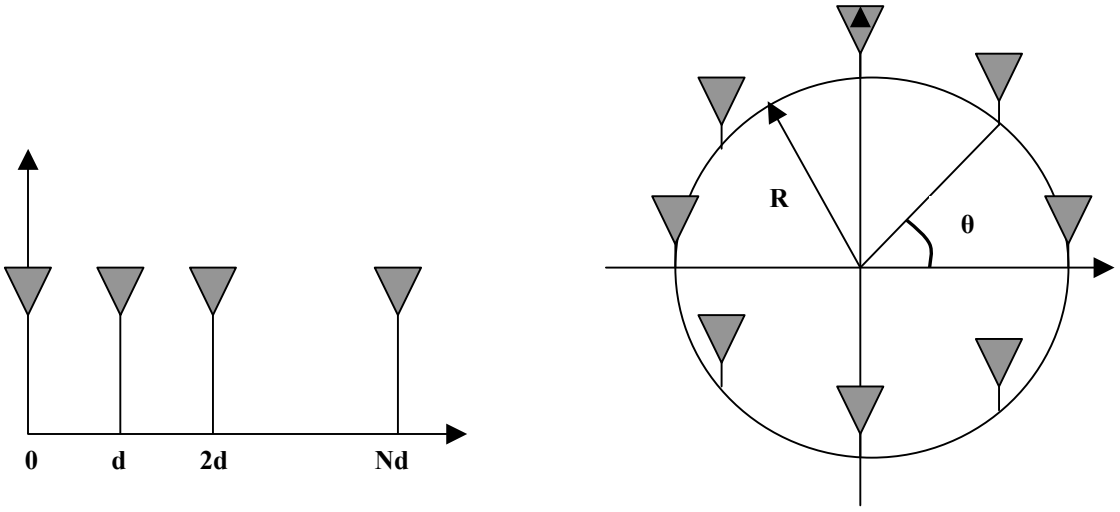

Figure 9. Common Antenna Array Geometries — Uniform Linear Array ULA (Left) and Uniform Circular Array UCA (right)

A. CHANNEL ILLUSTRATION

The vector channel model, $v(\theta)$, developed in Ref. [3] for an *N*-element ULA is shown below:

$$v(\theta) = \begin{bmatrix} 1 \\ e^{-j2\pi\frac{d}{\lambda}\sin(\theta)} \\ \vdots \\ e^{-j2\pi\frac{(k-1)d}{\lambda}\sin(\theta)} \end{bmatrix} \qquad k = 1, 2, \cdots, N. \tag{4.1}$$

where d is the separation distance between the array elements, θ is the angle of arrival of the desired signal, λ is the wavelength of the desired signal and N is the number of elements.

This model has been widely used to evaluate the performance of an adaptive antenna array in a mobile radio environment. In this thesis, the vector channel developed for

UCA is based on the same principle used in Ref. [3]. The array manifold vector $v(\theta)$ for a *N*-element UCA [7] is as follows:

$$v(\theta) = \begin{bmatrix} e^{-j2\pi\frac{R}{\lambda}\sin(\phi)\cos(\theta)} \\ e^{-j2\pi\frac{R}{\lambda}\sin(\phi)\cos\left(\theta-\frac{2\pi}{N}\right)} \\ \vdots \\ e^{-j2\pi\frac{R}{\lambda}\sin(\phi)\cos\left(\theta-\frac{2\pi(m-1)}{N}\right)} \end{bmatrix} \qquad m = 1, 2, \cdots, N, \tag{4.2}$$

where *R* is the circular radius of the antenna array, ϕ is the elevation angle (as in Figure 10), λ is the wavelength and *N* is the number of antenna elements. Without loss of generality, only the azimuth angles are considered in the propagation geometry, i.e., $\phi = 90^0$. The angle θ is on the horizontal plane where the arrays are positioned and measures from a reference imaginary axis on this horizontal plane. This thesis will analyze the impact of the angular spread on the interference-to-signal ratio (ISR) of the system, which in turn directly affects the performance of the UCA.

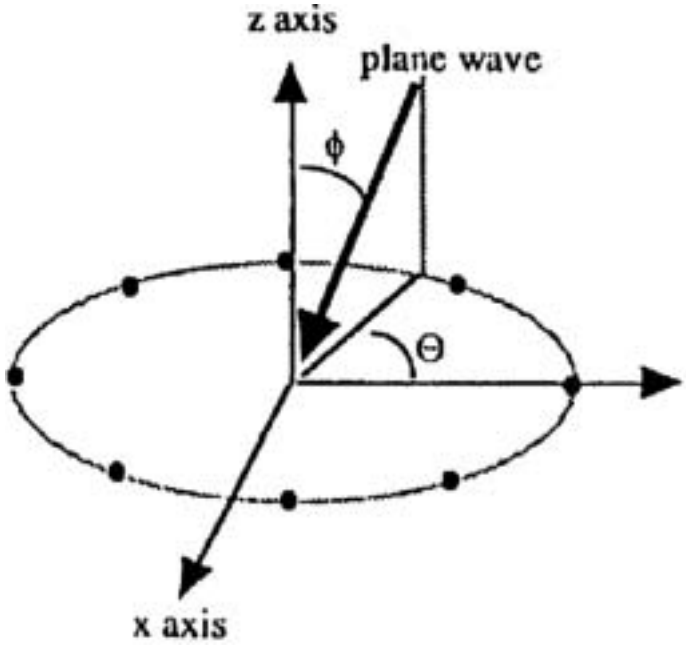

Figure 10. Uniform Circular Array Geometry

Contrasted with a switched-beam antenna with fixed directional beams, an adaptive antenna usually consists of an array with suitable inter-element spacing. The weights of each element of the antenna array are changed dynamically to minimize the signal-to-interference and noise ratio (SINR). Traditional adaptive antenna systems used in the military for radar and satellite applications make use of the well-defined AOA of the desired and interfering signals to determine the weights.

Basically, the weights are chosen so that the resulting antenna pattern will have nulls in the directions of the interfering signals and ideally a large maximum gain in the desired signal direction. An *N* element array will have *N-1* degrees of freedom. It can "null out" up to *N–1* interfering signals. Hence, the adaptive antenna can counteract against fading and co-channel interference and can increase system capacity.

Figure 11 shows an adaptive antenna array having *N* elements with *L* interfering signals. The received signal, x_k(t), at the *k*-th antenna element output is calculated as:

$$x_k(t) = s_k(t) + n_k(t), \quad k = 1, 2, 3, \ldots N. \tag{4.3}$$

Here, $s_k(t)$ is the complex signal envelope of the signal and $n_k(t)$ is the noise received by the *k*-th antenna element. From Equation (4.2), the complex signal envelope for the *N*-element in the UCA is calculated as follows:

$$s_k(t) = s(t)\, e^{j\frac{2\pi R}{\lambda}\cos\left(\theta - \frac{2\pi(k-1)}{N}\right)} \qquad k = 1, 2, \ldots, N, \tag{4.4}$$

where λ is the wavelength, θ is on the horizontal plane and $s(t)$ is the complex envelope of the transmitted desired signal.

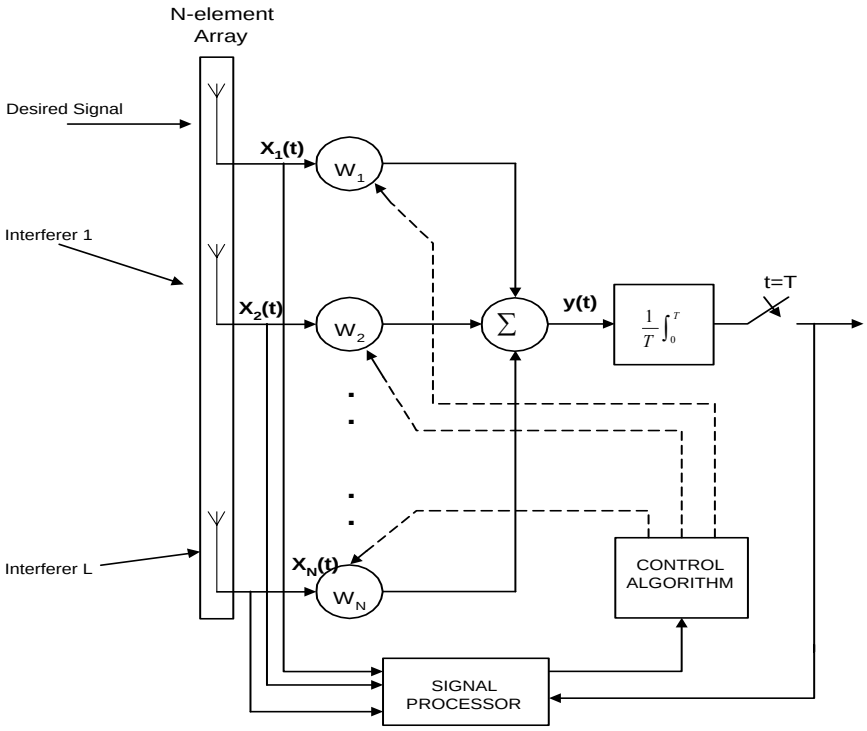

Figure 11. Block Diagram of an Adaptive Antenna System (From Ref. [1].)

Finally, the array output signal $y(t)$, which is the weighted sum of all the digitized input signals, $x_k(t)$, is determined from:

$$y(t) = \sum_{k=1}^{N} w_k x_k(t) = W^T X = X^T W, \tag{4.5}$$

where

$$W = \begin{bmatrix} w_1 \\ w_2 \\ \vdots \\ w_N \end{bmatrix}, \qquad X = \begin{bmatrix} x_1(t) \\ x_2(t) \\ \vdots \\ x_N(t) \end{bmatrix}. \tag{4.6}$$

The adaptive array system continuously adjusts the weights vector W by the optimum control algorithm with criterion such as Minimum Mean Square Error (MMSE) [1].

B. WEIGHTING OPTIMIZATION

Antenna array processing involves manipulating of the complex weighting of the signal induced on each antenna element in the array. This requirement necessitates independent amplitude and phase control at each array branch. In this respect, the phase control implementation is comparatively more straightforward than the amplitude control implementation. Conventionally, amplitude control can be achieved by a cascaded combination of amplifier and attenuator network

This thesis aims to minimize the ISR by using the algorithm to compute the optimal weight for the adaptive antenna system. A circular array with three to seven elements that is uniformly positioned in a circular pattern of radius R is used in the simulation. The general formula for the far-field antenna factor F_{array} that is calculated only for the azimuth angles in the propagation geometry is as follows:

$$F_{array} = \sum_{n=1}^{N} A_n e^{i\psi_n} e^{-j\frac{2\pi R}{\lambda}\cos\left(\theta - \frac{2\pi(n-1)}{4}\right)} \qquad \text{where } 3 \le N \le 7. \tag{4.7}$$

For example, in the instance of a four-element array, the amplitudes of the received signals are A_1, A_2, A_3 and A_4, and their individual phases are ψ_1, ψ_2, ψ_3 and ψ_4. As such, based on Equation 4.6, the far-field antenna factor F_{array} for a four-element array is calculated as follows:

$$\begin{aligned} F_{array} = {} & A_1 e^{i\psi_1} e^{-j\frac{2\pi R}{\lambda}\cos(\theta)} + A_2 e^{i\psi_2} e^{-j\frac{2\pi R}{\lambda}\cos\left(\theta - \frac{2\pi}{4}\right)} \\ & + A_3 e^{i\psi_3} e^{-j\frac{2\pi R}{\lambda}\cos\left(\theta - \frac{4\pi}{4}\right)} + A_4 e^{i\psi_4} e^{-j\frac{2\pi R}{\lambda}\cos\left(\theta - \frac{6\pi}{4}\right)}. \end{aligned} \tag{4.8}$$

Let the operating frequency be 2 GHz and the circular radius R of the antenna element to be $\lambda/2$, coupled with the normalized total power (gain) to be equal to 1 by using a relationship of $A_1^2 + A_2^2 + A_3^2 + A_4^2 = 1$. This will generate any far field antenna factor in any of the 360^0 azimuth.

The directions of arrival (DoA) of the desired-signal ϕ_b (base-station) and the interference signals ($\phi_{i1}, \phi_{i2}, \phi_{i3}$) can be estimated. With these DoA estimated, if we take the desired base-station signal as a reference, the complex gains of the array in the direction of the desired signal F_{array_b} and the three interferers ($F_{array_{i1}}, F_{array_{i2}} F_{array_{i3}}$) can be defined as:

$$F_{array_b} = A_1 e^{j\frac{2\pi R}{\lambda}\cos(\theta_b)} + A_2 e^{i\psi_1} e^{-j\frac{2\pi R}{\lambda}\cos\left(\theta_b - \frac{2\pi}{4}\right)} + A_3 e^{i\psi_2} e^{-j\frac{2\pi R}{\lambda}\cos\left(\theta_b - \frac{4\pi}{4}\right)} + A_4 e^{i\psi_3} e^{-j\frac{2\pi R}{\lambda}\cos\left(\theta_b - \frac{6\pi}{4}\right)}, \tag{4.9}$$

$$F_{array_{i1}} = A_1 e^{-j\frac{2\pi R}{\lambda}\cos(\theta_{i1})} + A_2 e^{i\psi_1} e^{-j\frac{2\pi R}{\lambda}\cos\left(\theta_{i1} - \frac{2\pi}{4}\right)} + A_3 e^{i\psi_2} e^{-j\frac{2\pi R}{\lambda}\cos\left(\theta_{i1} - \frac{4\pi}{4}\right)} + A_4 e^{i\psi_3} e^{-j\frac{2\pi R}{\lambda}\cos\left(\theta_{i1} - \frac{6\pi}{4}\right)}, \tag{4.10}$$

$$F_{array_{i2}} = A_1 e^{-j\frac{2\pi R}{\lambda}\cos(\theta_{i2})} + A_2 e^{i\psi_1} e^{-j\frac{2\pi R}{\lambda}\cos\left(\theta_{i2} - \frac{2\pi}{4}\right)} + A_3 e^{i\psi_2} e^{-j\frac{2\pi R}{\lambda}\cos\left(\theta_{i2} - \frac{4\pi}{4}\right)} + A_4 e^{i\psi_3} e^{-j\frac{2\pi R}{\lambda}\cos\left(\theta_{i2} - \frac{6\pi}{4}\right)}, \tag{4.11}$$

$$F_{array_{i3}} = A_1 e^{-j\frac{2\pi R}{\lambda}\cos(\theta_{i3})} + A_2 e^{i\psi_1} e^{-j\frac{2\pi R}{\lambda}\cos\left(\theta_{i3} - \frac{2\pi}{4}\right)} + A_3 e^{i\psi_2} e^{-j\frac{2\pi R}{\lambda}\cos\left(\theta_{i3} - \frac{4\pi}{4}\right)} + A_4 e^{i\psi_3} e^{-j\frac{2\pi R}{\lambda}\cos\left(\theta_{i3} - \frac{6\pi}{4}\right)}. \tag{4.12}$$

The amplitude of the received signal is calculated as:

$$A_4 = \sqrt{A_1^{\,2} + A_2^{\,2} + A_3^{\,2}}, \tag{4.13}$$

and, the ISR can be defined as:

$$ISR = \frac{\sqrt{\left|F_{array_{i1}}\right|^2 + \left|F_{array_{i2}}\right|^2 + \left|F_{array_{i3}}\right|^2}}{\left|F_{array_b}\right|}. \tag{4.14}$$

In order to optimize the complex weights that include both amplitude and phase values and to minimize the interference, constraint minimization of the ISR was performed by using minimization functions from Matlab. These minimization functions allow one to search for optimized solutions for a non-linear function with some estimating of the initial values. To ensure that the weights amplitude conform to our normalization of gain power, we place constraints of $0 < A_{1,}, A_2, A_3 < 1$.

In the case of the four-element array, there would be six unknown variables $(A_1, A_2, A_3, \psi_1, \psi_2, \psi_3)$ to be optimized, which effectively perform the null steering for the three interferers. The most optimum strategy is to steer the null toward the interferer first rather than trying to maximize the gain of the desired signal beam. The initial guesses of the values of the six variables are as follows:

$$A_1 = A_2 = A_3 = \frac{1}{\sqrt{4}}; \quad \psi_1 = \psi_2 = \psi_3 = \frac{\pi}{4}. \tag{4.15}$$

With the optimum weight values obtained after minimizing the ISR, these weights are back-substituted into Equations (4.14) to compute the optimum ISR (ISR_{opt}) and to obtain the antenna factor values for all directions.

C. CIRCULAR ARRAY CHARACTERISTICS

1. Radiation Pattern

The radiation pattern is a graphical representation of the radiation properties of the antenna as a function of space coordinates. As mentioned above, the antenna array has the ability to adapt the radiation pattern to the current scenario. Each antenna element in the antenna array has its own fixed radiation pattern. In this thesis, each antenna element is assumed to be an isotropic radiator; each antenna element has equal radiation in all directions. When transmitting, the radiation pattern of the antenna represents the power distribution for all directions. When receiving, the radiation pattern represents the sensitivity in different directions. The radiation pattern contains a number of lobes that have different shapes and sizes. The lobes can be divided into major, side and back lobes as shown in Figure 12. The major lobe (blue arrow), also called the main beam, repre-

sents the direction of maximum radiation, which is the direction where the output power is highest. Any lobe beside the main beam is a side lobe (yellow arrow) and has a direction other than the main beam. Finally, the lobe with a direction opposite to the main beam is called the back lobe (black arrow). A trade off between the main beam and the side lobes must be made. For example, by allowing a wider main beam, the side lobes can be reduced. Minimizing the side lobes is often desirable since they usually represent radiation in undesired directions. The level of the side lobes is usually expressed as a ratio of the power density in the lobe in question to the major lobe. Finally, the output power is very low between the lobes and these directions are defined as the null directions (red arrow).

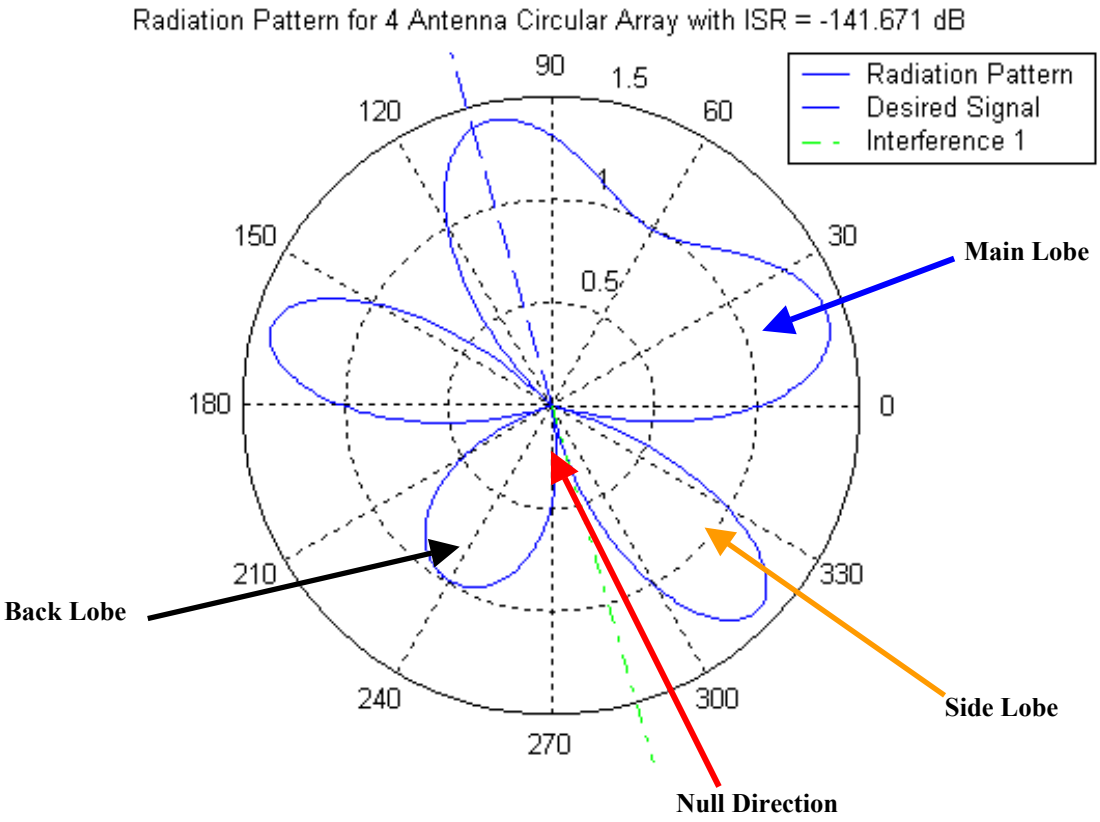

Figure 12. Radiation Pattern of a Four-Antenna Circular Antenna Array.

2. Antenna Angular Spread and Spacing

The angular spread between the desired and interferer signals must be sufficiently large so that they do not affect the functionality of the entire system. If the angular spread between the desired signal and the interferer is too small, the antenna array may not be able to discriminate the interferer signal with deep nulls unless the antenna among element-to-element separation is increased. As such, placing the antenna elements a half wavelength of the radio signal apart from each other to avoid these ambiguities is preferable.

Consequently, the size of the antenna array depends on the frequency used, since the frequency is proportionally related to the wavelength. The number of antenna elements used directly affects the radiation pattern of the antenna array. Generally, adding additional antenna elements enhances the possibility of suppressing interferers due to the increased number of null directions. In addition, the more antenna elements that are used, the narrower the shape of the major lobe becomes, and this gives a higher antenna gain. Antenna arrays therefore function better at high frequencies because this implies that more antenna elements can be used, without increasing the dimension of the antenna array.

With the optimum complex weights determined for the adaptive antenna system, it was noted that the depth of the null steer for suppressing interference depends on the geometry scenarios between the angular spread of the desired signal and interferers' direction-of-arrival (DoA), the antenna-array arrangement and separation, and the geometric orientation between the array and all the other sources. All these factors contribute to the complexity of the operating environment and make it more difficult to ensure a minimum required system performance.

The characteristics and constraints of a circular-adaptive array were presented in this Chapter. The next Chapter will present the performance analysis of the adaptive antenna system in a circular pattern for the forward channel model of the DS-CDMA system.

V. PERFORMANCE ANALYSIS OF ADAPTIVE ANTENNA SYSTEM IN A CIRCULAR PATTERN

This Chapter analyses the performance of an adaptive antenna system in a circular pattern. The forward channel propagation model of a DS-CDMA mobile communication system in a slow, flat Rayleigh fading and Nakagami-m log-normal shadowing environment is also presented in this Chapter as most data services are asymmetric, with the downstream requiring a higher data rate more frequently.

A. PATH LOSS COMPONENTS

The mobile user can be located anywhere within the cell, with two degrees of freedom because its position can be at distance R from its base station and can be at a particular angle to the base station. The three basic components of the path loss model are as follows:

(1) Loss proportional to the power law, which is due to the radiation of the RF signal through space. This is the loss in the empirically derived Hata model [2].

(2) Variable loss caused by shadow fading is modeled as log-normal shadowing.

(3) Variable loss caused by multi-path fading. Multi-path fading occurs when signals that have traveled over many different paths from the transmitter are received. The variations in signal level resulting from multi-path fading is modeled by a Nakagami-m probability distribution.

1. Hata Model

The Hata Model is the analytical expression of the Okumura empirical model, which is one of the most accurate empirical models in cellular communications [2]. This model is valid for the 500-1500 MHz frequency range with receiver distances greater than 1 km from the base station and with base station antenna heights greater than 30 m. The Hata model computes the median path loss in an urban environment and supplies correction equations in order to be applicable to other situations. An elaboration on the

Hata-Okumura model can extend the carrier frequency range from 1,500 MHz to 2,000 MHz [2]. However, these models are not suitable for smaller base station antenna heights, larger receiver antenna heights, and hilly or heavily wooded terrain. The original Hata model matches the Okumura model closely for distances greater than 1 km, and the extended model [2] further extends to cover higher frequency ranges with distances of about 1 km. In this thesis, the extended model better represents the operating environment of a 3G cellular system.

The extended Hata model, which predicts the median path loss L_H in dB as defined in Ref. [2] by

$$\begin{aligned} L_H &= 46.3 + 33.9 \log f_c - 13.92 \log h_{base} - a(h_{mobile}) \\ &\quad + (44.9 - 6.55 \log h_{base}) \log d + C_M . \end{aligned} \tag{5.1}$$

where

$$a(h_{mobile}) = \left[1.1 \log\left(f_c\right) - 0.7\right] h_{mobile} - \left[1.56 \log\left(f_c\right)\right]. \qquad (\text{dB}) \tag{5.2}$$

and

$$C_M = \begin{cases} 0 \text{ dB for medium sized city and suburban areas} \\ 3 \text{ dB for metropolitan areas.} \end{cases}$$

Note that

f_c : carrier frequency in MHz,

h_{base} : base-station antenna height in meters (m),

h_{mobile} : mobile-station antenna height in meters (m), and

d : separation distance is measured in kilometers (km).

The extended Hata model is restricted to the following range of parameters:

f_c : 1,500 MHz to 2,000 MHz,

h_{base} : 30 m to 200 m,

h_{mobile} : 1 m to 10 m, and

d : 1 km to 20 km.

The mobile and base-station heights of 1 m and 30 m, respectively, with an operating carrier frequency of 2,000 MHz were chosen for this thesis. As such, based on the Hata path loss model, the main factors can be summarized as follows:

(i) *The Environment*: An example built up or urban areas, suburban and rural areas all effect the propagation of radio signals differently.

(ii) *Signal Frequency*: This has a direct impact on the propagation loss. The higher the frequency the greater the propagation loss.

(iii) *Antenna Height*: The height of both the base station and the mobile antenna impact the propagation loss. In a mobile environment, we can assume that line of sight propagation is rare. This means that generally the mobile is shadowed from the base station by the surrounding environment (buildings, trees, etc.). Therefore, by reducing the loss by raising the base station antenna above the surrounding obstacles is possible. A similar argument applies for the mobile antenna. Of course in practice there are limits to what can be achieved for mobile communications.

2. Log-normal Shadowing

The average path loss is a function of the path loss exponent n and is given in dB The environment may differ a lot at two separate points, which have the same distance d from the transmitter. It can be stated that the previous equation does not predict with accuracy the path loss at these two different points [2]. This happens because the terrain variations in a particular path can result in a path loss that is significantly different from the predicted average path loss. A Gaussian random variable χ with zero-mean and σ_{dB} standard deviation can be used to represent the shadowing of the average path loss value. The path loss with shadowing accounted for is modeled by

$$L_X(D) = L_H(d) + \chi, \quad \text{(dB)} \tag{5.3}$$

where $L_H(D)$ is the average path loss at distance D km.

The above equation can be converted to a log-normal random variable L_X as defined in Ref. [3]

$$L_X = L_H X. \tag{5.4}$$

The above log-normal random variable L_X in Equation 5.4, which accounts for the effect of log-normal shadowing with the Hata model, can then be applied to the signal in the forward channel of the DS-CDMA cellular system in a Nakagami-m slow-flat fading environment. In summary, the three basic propagation mechanisms can be further classified as follows:

(i) *Reflection*: This is where the signal is reflected from a low-loss surface that is larger than the wave length of the propagating wave and continues to propagate essentially in a single direction.

(ii) *Diffraction*: This is where the signal wavefront "bends" as it hits the edge of sharp irregularities, for example a building or a roof.

(iii) *Scattering*: Scattering occurs when the signal wavelength is large relative to the size of the objects that it encounters or where many small objects or irregularities exist.

3. Multi-path Fading

Multi-path has been mentioned a number of times now so an explanation of this should be discussed. In mobile and portable radio channels there are multiple radio paths between transmitter and receiver as shown in Figure 13. The longer paths result in delayed versions of the desired signal arriving at the receiver and, if this delay is large, the data symbols spread into one another, leading to inter-symbol interference (ISI) at the receiver. This can result in poor signal reception, and even with a small time delay spread, fading of the received signal level may occur.

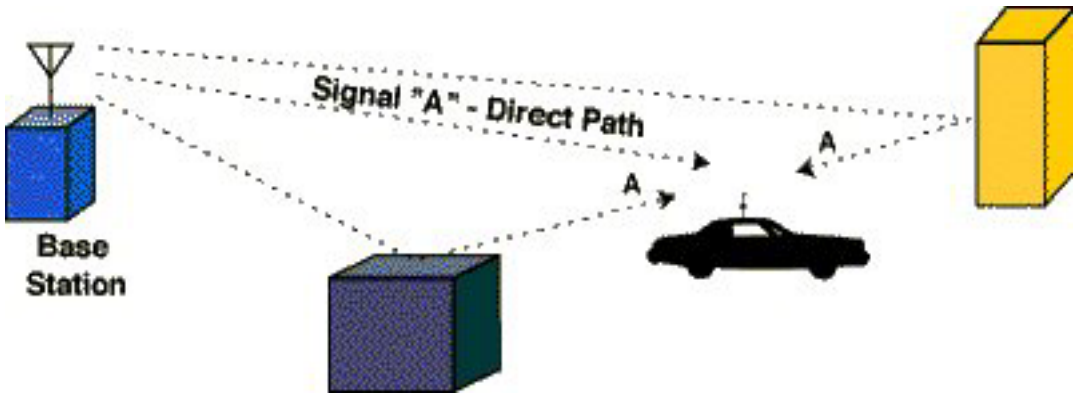

Figure 13. Multi-path Effects

The signal fluctuations that occur over sub-wavelengths have already been defined and are known as fast fading or small-scale fading [2], due to the multi-path reception of a wireless signal. Many signal copies arrive at the receiver at different time intervals because they follow different propagation paths or because in a wireless environment either transmitter or receiver moves with time. (This is why there is a Doppler-shift in the frequency of the transmitted signal.) The fact that the receiver will or will not be able to receive each information data bit or symbol correctly depends on the small-scale fading characteristics of the channel and the signal characteristics itself. In Ref. [2], a classification of types of small-scale fading occurs due to two independent facts, such as multi-path delay spread and Doppler spread. Figure 14 shows a tree of the four different types of fading [2]. For the case of flat fading, the bandwidth of the signal is smaller than the bandwidth of the channel causing deep fades, and thus may require 20 dB more transmitter power to achieve low and bit error rates.

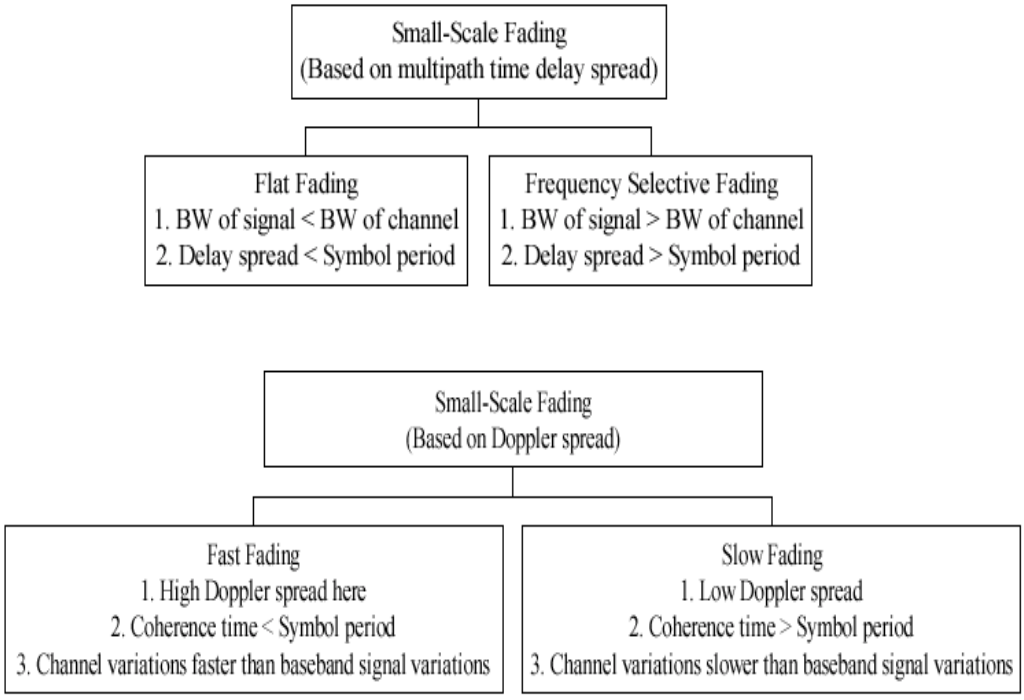

Figure 14. Types of Small-Scale Fading (From Ref. [2])

In reality, fast fading environments have only been observed in communication systems with very low data rates [2]. Since high data rates will be used in this thesis, the model is characterized as slow fading. A general method for modeling the amplitude variations in a flat fading channel is by assuming that the amplitudes are distributed as a Nakagami random variable. As a result, the forward channel propagation model of a DS-CDMA mobile communication system is a slow, flat Rayleigh fading and Nakagami-m log-normal shadowing environment.

B. PERFORMANCE ANALYSIS FOR CIRCULAR ADAPTIVE ARRAY

The Rayleigh-log-normal channel model is then applied to a typical DS-CDMA cellular system consisting of traffic from a cell's base station to the mobile users in the

cell, which characterize the received signal of a mobile user. This received signal includes both traffic intended for the mobile user from the Signal Base-Station (SBS), traffic from other users in the cell (intra-cell interference), traffic for users in adjacent cells (inter-cell interference) and additive white noise.

Subsequently, the performance on the forward channel with equally spaced circular smart antenna arrays at the mobile user within the cell is being assessed in this chapter. Analyzing the forward channel with an adaptive array is complex, as the channel is wireless, the position of the user is mobile, and the orientation of the array is random. As discussed earlier, the DS-CDMA forward channel model developed in Ref. [4], for a received signal at the mobile user in a Rayleigh log-normal channel was used in this analysis. Since thousands of possible locations can exist within the cell, and since each position can have random orientations that affect the circular antenna array ISR, evaluating the overall system BER performance can be extremely computationally expensive. As in Ref. [5], this thesis adopts a four-boundary approach to better represent the adaptive-array system's performance for evaluating and comparing it to a system without a smart antenna.

In Ref. [5], the performance boundary for a three- and four- element linear array were examined by positioning the Mobile Station (MS) randomly within the cell, with the MS being rotated 360^0 at each location. The adaptive array optimization for each random MS position at each orientation was further assessed with 1^0 resolution for the whole 360^0 orientation. For each of the optimized weights obtained for each 1^0 orientation, the optimized weights were used to compute the antenna gain for the antenna-array factors. The best and worst path-loss ratio that correspond to the best and worst system performance for that single location were selected. The random position was confined to fall within the 60^0 sector, as the hexagonal cell is symmetrical in all such 60^0 sectors and the performance analysis on one of the 60^0 sectors could apply to all the cells without losing any generality. The four boundaries are defined as follows:

1. Best of Best boundary (BB)
2. Worst of Best boundary (WB)

3. Worst of Worst boundary (WW)

4. Best of Worst boundary (BW)

In this thesis, the circular antenna array was optimized over a 360^0 orientation for any mobile user positions within the center cell of a 7-cell cluster, based on the similar method that was developed in Ref. [5]. The interferer-signal-ratio (ISR) factor will be used to illustrate the effectiveness of the UCA with a different number of array elements and interferers respectively based on the random locations of the WB boundary. As stated in Ref. [5], the WB boundary gives a good indication of the performance of the system. This boundary also indicates the worst case of the best performance achieved by the system with an adaptive array coupled with 360^0 of freedom.

The next few plots from Figure 15 to Figure 19, using Matlab simulations, exhibit how UCA combats interference using a different number of array elements to produce an antenna pattern to nullify the interferers.

Figure 15 shows the radiation pattern for a three-element UCA with 2 interferers at 15^0 and 110^0, respectively. UCA is able to combat interference and produce an interference-to-signal ratio (ISR) of –113.495 dB. Figure 16 shows the radiation pattern of a four-element UCA with 2 interferers and it performed better than the three-element UCA by 19.26 dB in terms of ISR. However, this is done with a cost of an addition element array. Nevertheless, when an additional interferer is added to the four-element UCA, the ISR degrade to –107.652 dB as shown in Figure 17.

Figure 18 shows the radiation pattern of a five-element UCA with 4 interferers and it managed to achieve an ISR of –97.258 dB. Similarly, Figure 19 illustrates the radiation pattern of a six-element UCA with 5 interferers and it managed to accomplish an ISR of –103.243 dB.

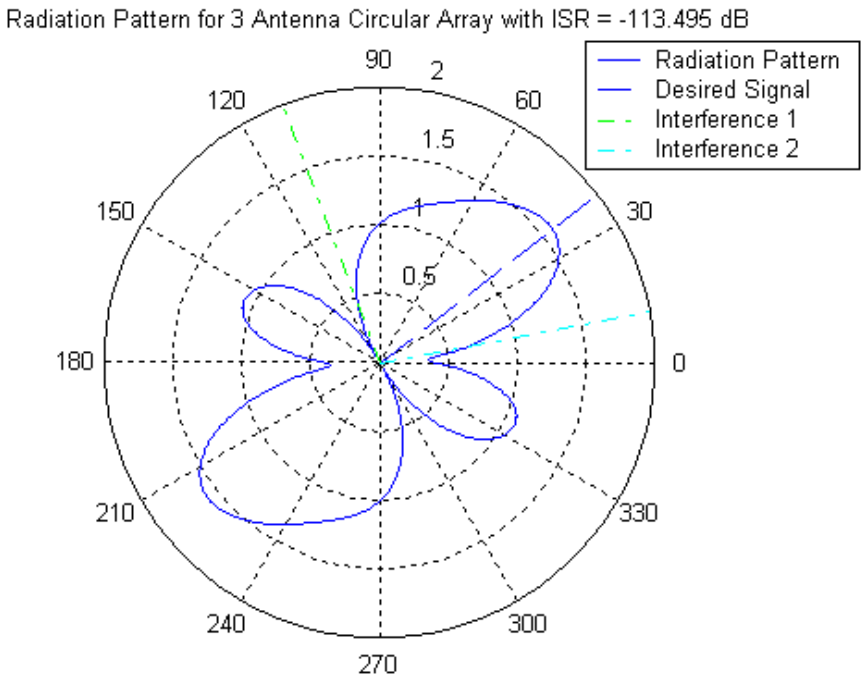

Figure 15. Radiation Pattern for a Three-Element Circular Array with 2 Interferers

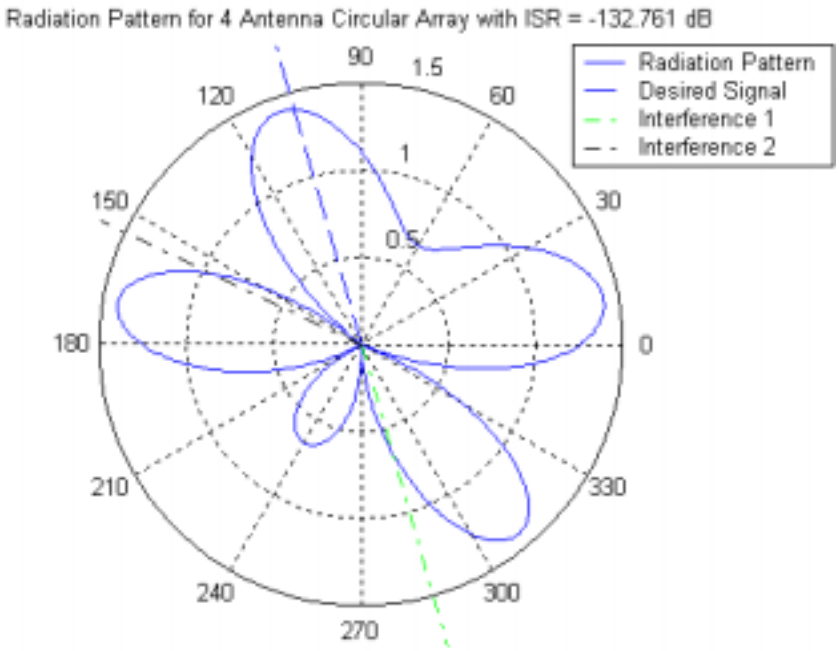

Figure 16. Radiation Pattern for a Four-Element Circular Array with 2 Interferers

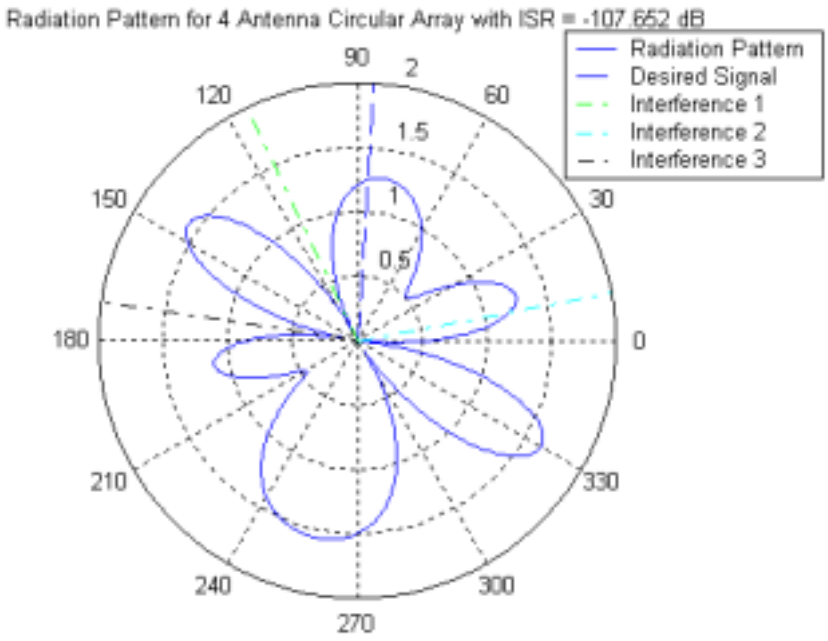

Figure 17. Radiation Pattern for a Four-Element Circular Array with 3 Interferers

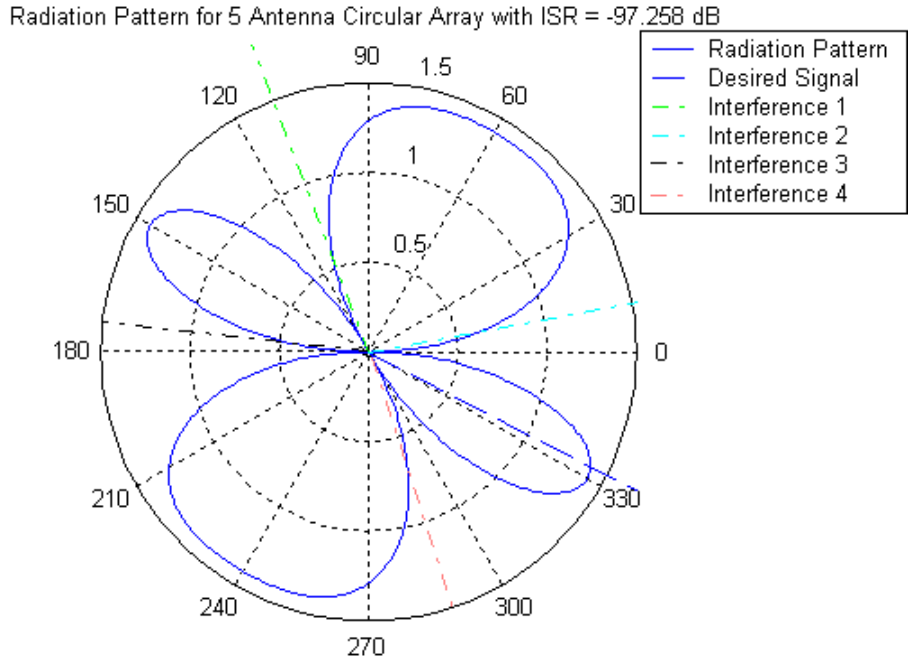

Figure 18. Radiation Pattern for a Five-Element Circular Array with 4 Interferers

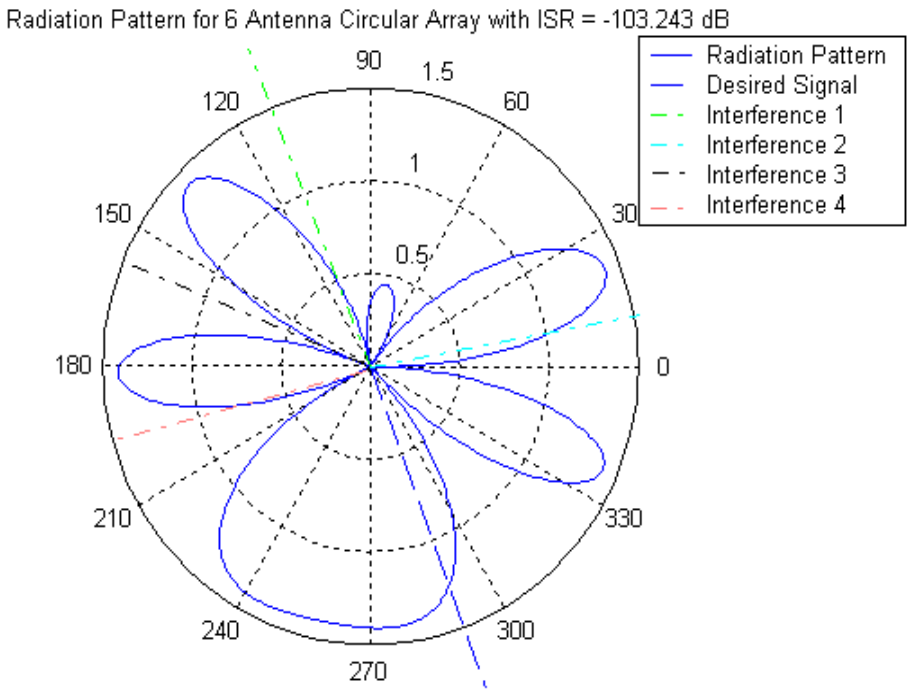

Figure 19. Radiation Pattern for a Six-Element Circular Array with 4 Interferers

From Table 1, it is clear that UCA has the ability to combat interference with of using weights are chosen so that the resulting antenna pattern will have nulls in the directions of the interfering signals and ideally a large maximum gain in the desired signal direction. An *N* element array will have *N-1* degrees of freedom. It can "null out" up to *N–1* interfering signals. Hence, the adaptive antenna can counteract against fading and co-channel interference and can increase system capacity.

A summary of the simulation results of UCA with a different number of elements and associated interferers respectively in terms of ISR are exemplified in Table 1:

Interferers / UCA Elements		2	3	4	5
	–138.216dB	–113.495dB	NA	NA	NA
4	–141.671dB	–132.761dB	–107.652dB	NA	NA
5	–141.983dB	–134.562dB	–110.254dB	–97.258dB	NA
6	–142.117dB	–134.933dB	–112.792dB	–101.243dB	–96.781dB
7	–142.065dB	–136.083dB	–114.623dB	–102.325dB	–96.975dB

Table 1. Simulation Results Using UCA with a Different Number of Elements and the Associated Interferers

In Ref. [3], both large-scale and small-scale propagation effects are combined into a single model. This combined Nakagami-m log-normal channel fading model will characterize the mobile radio channel accurately in a single unified model that can more completely analyze the mobile radio channel.

The Nakagami-m log-normal channel model is then applied to a typical DS-CDMA cellular system consisting of traffic from a cell's base station to the mobile users in the cell, which characterizes the received signal for a mobile user. This received signal includes both traffic intended for the mobile user from the Signal Base-Station (SBS), traffic from other users in the cell (intra-cell interference), traffic for users in adjacent cells (inter-cell interference) and additive white noise.

The Signal-to-Noise plus Interference Ratio (SNIR) and Bit Error Rate (BER) for the DS-CDMA forward channel in the Rayleigh-lognormal fading channel were derived

in Ref. [3]. Using the formula that was developed in Ref. [3], the bit error probability P_b is given as:

$$P_b = Q\left(\sqrt{\frac{Z}{\alpha}}\right), \tag{5.5}$$

where Z is the Nakagami-square-lognormal random variable, and

$$Z = R^2 \tilde{X}. \tag{5.6}$$

Hence,

$$P_b = Q\left(\sqrt{\frac{R^2 \tilde{X}}{\alpha}}\right), \tag{5.7}$$

and [4, Eq. 4.60]

$$\alpha = \frac{e^{\left(\frac{\lambda^2 \sigma_{dB}^2}{2}\right)}}{3N} \sum_{i=1}^{6} \sum_{j=0}^{K_i - 1} \frac{L_H(D)}{L_H(D_i)} + \frac{N_o}{2E_b}. \tag{5.8}$$

From the above equations, the random variable *Z* is a Nakagami-square-lognormal random variable. As such, this thesis further demonstrates the WB boundary performance of the DS-CDMA systems with a three- and four- element array respectively in order to illustrate the effectiveness of the UCA without the use of coding.

As stated earlier in this chapter, σ_{dB} is a standard deviation that can be used to represent the shadowing of the average path loss value. Therefore, increasing this value will symbolize a hasher environment and thus reduce the effectiveness of the adaptive antenna. The next few plots from Figure 20 to Figure 31 show the simulation results and the comparison between the UCA and the ULA for the WB boundary that includes the average SNR per bit for a different number of active mobile users.

For a given level of BER and a number of active users, the corresponding average SNR per bit can be determined for each configuration, namely:

a) σ_{dB} = 7, 8 and 9; for a three- and four- element ULA

b) σ_{dB} = 7, 8 and 9; for a three- and four- element UCA

Figures 20 and 21 illustrate the performance for the DS-CDMA System with a three-element ULA and UCA, respectively, with $\sigma_{\mathrm{dB}} = 7$ for $N = 128$ in a Rayleigh Fading Channel. It is clear that for a given value of P_b the UCA performs better than ULA. For example, at $P_b = 10^{-1}$ and 20 users per cell, ULA requires a SNR per bit of 13 dB as compared to UCA that requires only a SNR per bit of 11 dB.

Figures 22 and 23 illustrate the performance for the DS-CDMA System with a three-Element ULA and UCA, respectively, with $\sigma_{\mathrm{dB}} = 8$ for $N = 128$ in a Rayleigh Fading Channel. As σ_{dB} is increased to 8, this symbolized that the system is operating in a hasher environment and thus reduces the effectiveness of the adaptive antenna. It is evident that for a given value of P_b, the UCA performs better than ULA. For example, at $P_b = 10^{-1}$ and 20 users per cell, ULA requires a SNR per bit of 17 dB as compared to UCA that requires only a SNR per bit of 14 dB. Figures 24 and 25 further reveal the performance for the DS-CDMA System with a three-element ULA and UCA, respectively, with $\sigma_{\mathrm{dB}} = 9$ for $N = 128$ in a Rayleigh Fading Channel. Clearly, the performance of the system is degraded under a hasher fading environment.

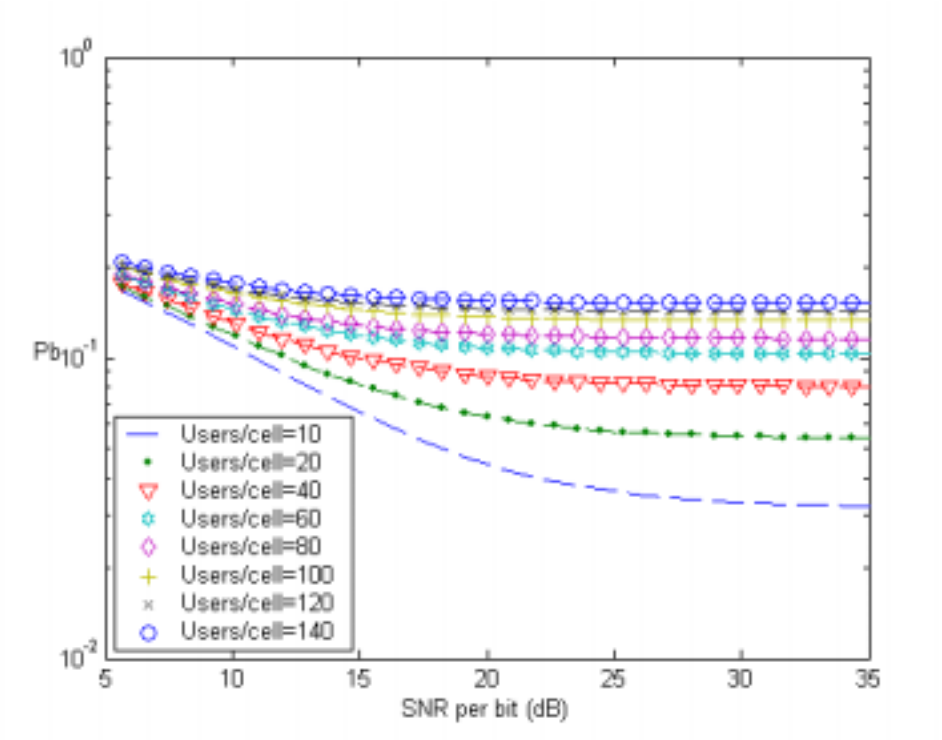

Figure 20. Performance for the DS-CDMA System with a Three-Element ULA ($\sigma_{\text{dB}} = 7$) for $N = 128$ in a Rayleigh Fading Channel

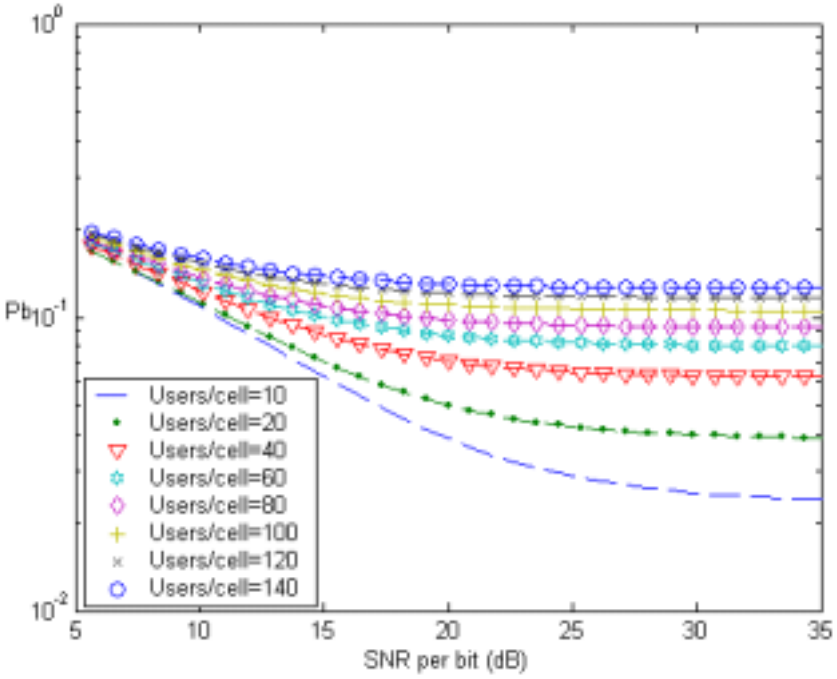

Figure 21. Performance for the DS-CDMA System with a Three-Element UCA ($\sigma_{\text{dB}} = 7$) for $N = 128$ in a Rayleigh Fading Channel

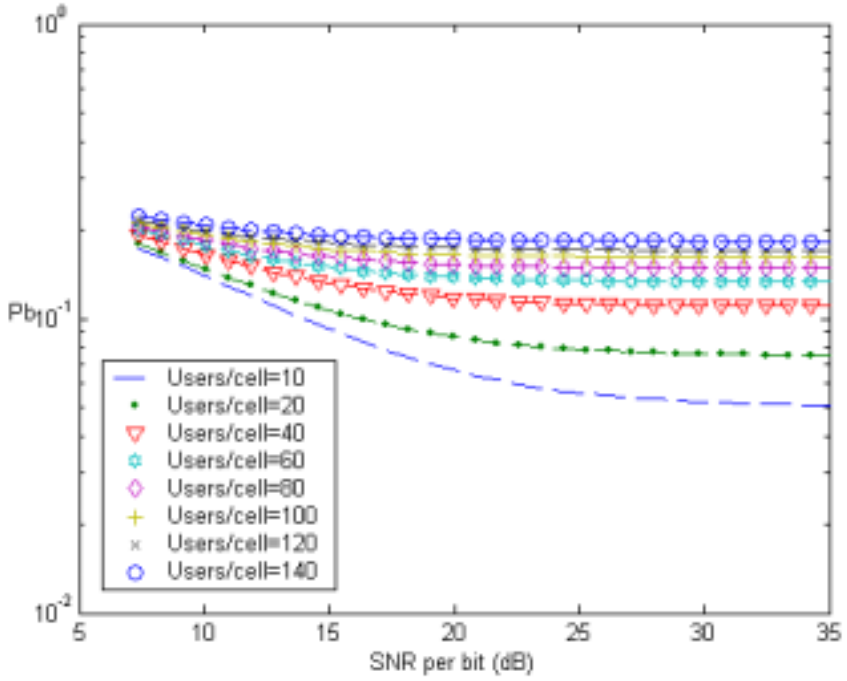

Figure 22. Performance for the DS-CDMA System with a Three-Element ULA ($\sigma_{\text{dB}} = 8$) for $N = 128$ in a Rayleigh Fading Channel

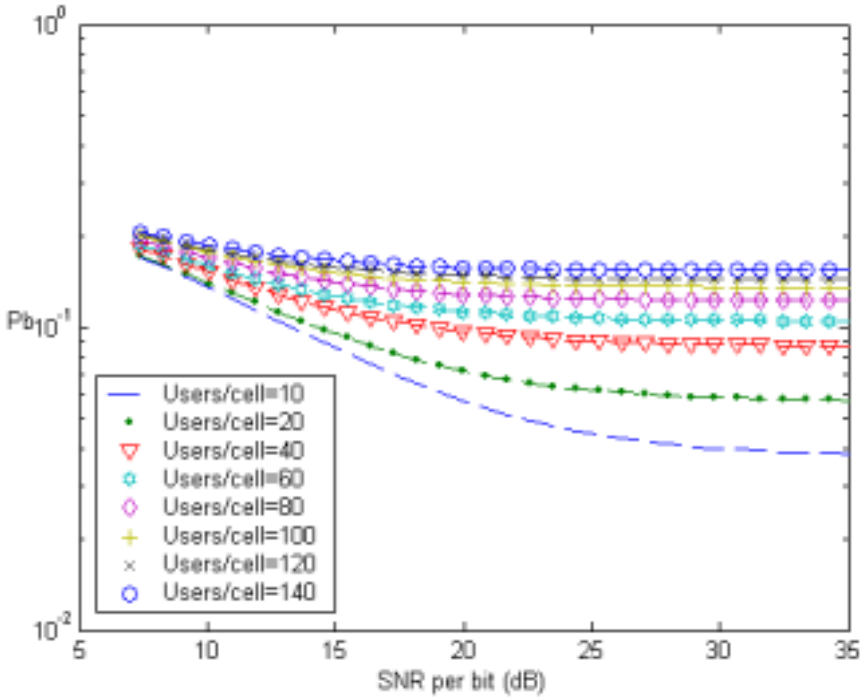

Figure 23. Performance for the DS-CDMA System with a Three-Element UCA ($\sigma_{\text{dB}} = 8$) for $N = 128$ in a Rayleigh Fading Channel

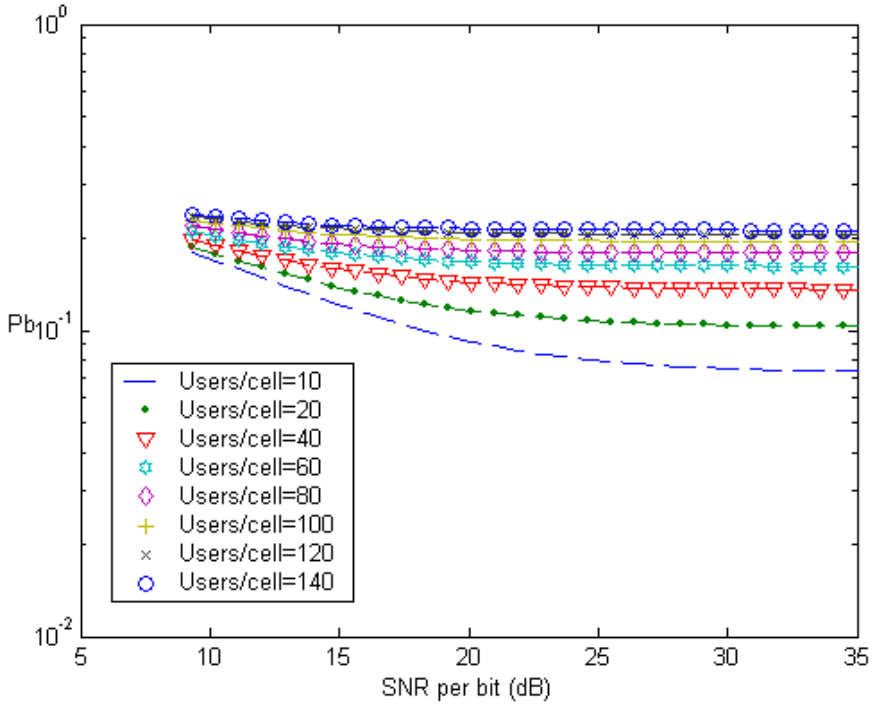

Figure 24. Performance for the DS-CDMA System with a Three-Element ULA ($\sigma_{\text{dB}} = 9$) for $N = 128$ in a Rayleigh Fading Channel

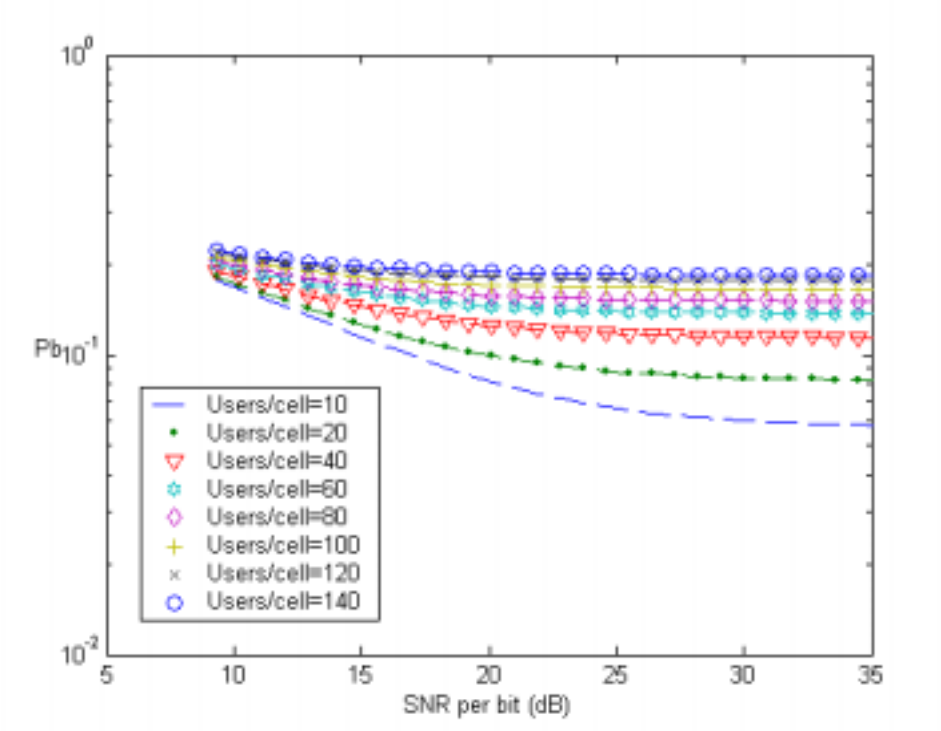

Figure 25. Performance for the DS-CDMA System with a Three-Element UCA ($\sigma_{\text{dB}} = 9$) for $N = 128$ in a Rayleigh Fading Channel

Figures 26 and 27 illustrate the performance for the DS-CDMA System with a four-element ULA and UCA, respectively, with $\sigma_{\text{dB}} = 7$ for $N = 128$ in a Rayleigh Fading Channel. It is evident that for a given value of P_b the UCA performs better than ULA. For example, at $P_b = 10^{-2}$ and 10 users per cell, ULA requires a SNR per bit of 17 dB as compared to UCA that requires only a SNR per bit of 15 dB.

Figures 28 and 29 illustrate the performance for the DS-CDMA System with a four-element ULA and UCA, respectively, with $\sigma_{\text{dB}} = 8$ for $N = 128$ in a Rayleigh Fading Channel. As σ_{dB} is increased to 8, this corresponds to that the system operating in a more severe fading environment and thus reduces the effectiveness of the adaptive antenna. It is evident that for a given value of P_b, the UCA performs better than ULA. For example, at $P_b = 10^{-2}$ and 10 users per cell, ULA requires a SNR per bit of 26 dB as compared to UCA that requires only a SNR per bit of 20 dB. Figures 30 and 31 further reveal the performance for the DS-CDMA System with a four-element ULA and UCA, respectively, with $\sigma_{\text{dB}} = 9$ for $N = 128$ in a Rayleigh Fading Channel. Clearly, the performance of the system is degraded under a hasher fading environment.

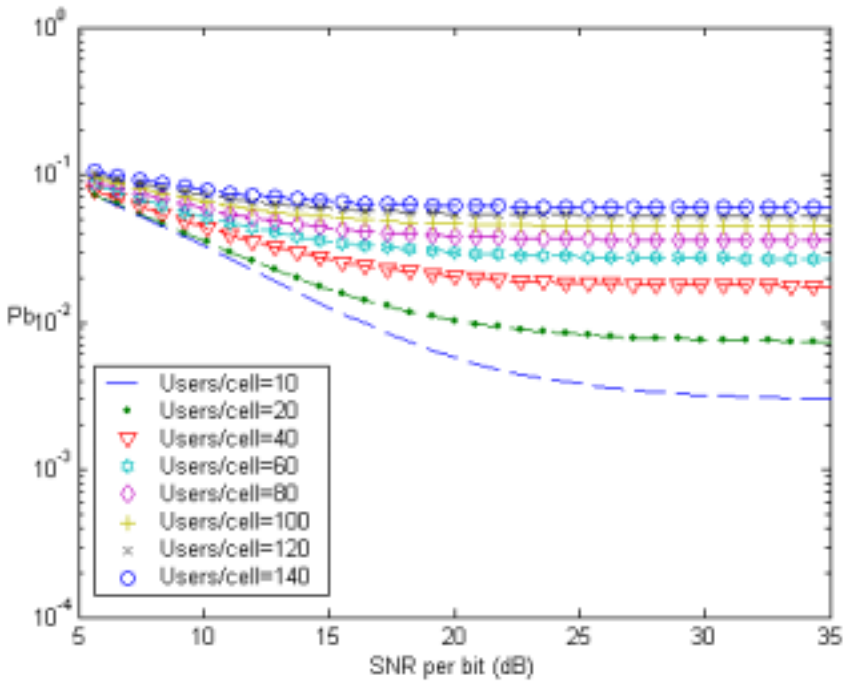

Figure 26. Performance for the DS-CDMA System with a Four-Element ULA ($\sigma_{dB} = 7$) for $N = 128$ in a Rayleigh Fading Channel

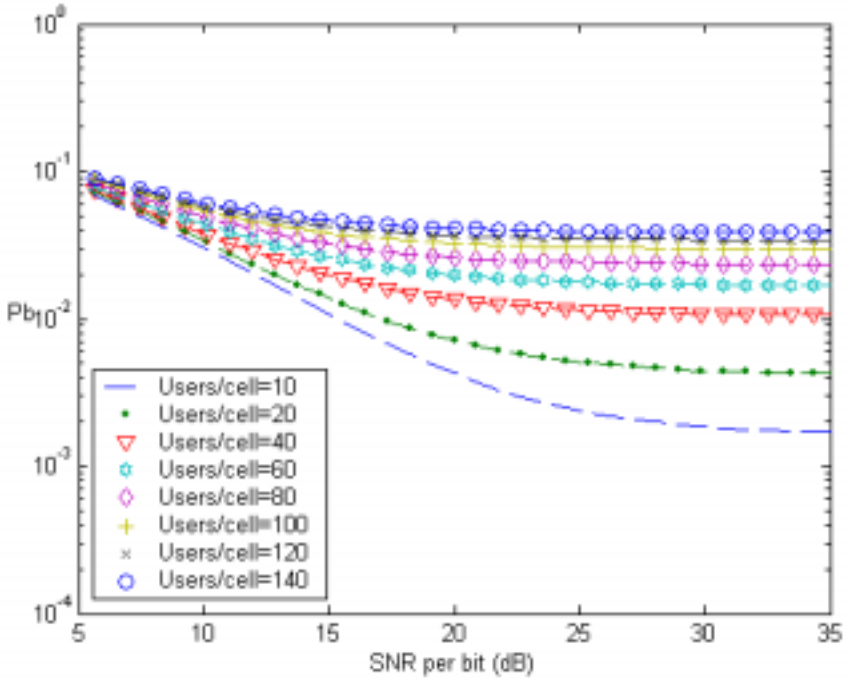

Figure 27. Performance for the DS-CDMA System with a Four-Element UCA ($\sigma_{dB} = 7$) for $N = 128$ in a Rayleigh Fading Channel

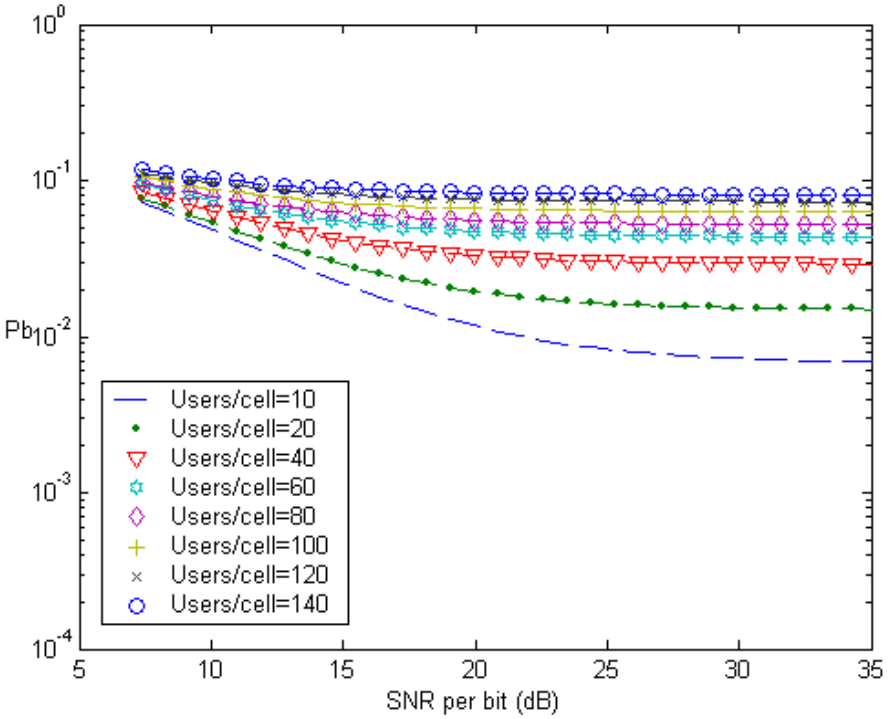

Figure 28. Performance for the DS-CDMA System with a Four-Element ULA ($\sigma_{\text{dB}} = 8$) for $N = 128$ in a Rayleigh Fading Channel

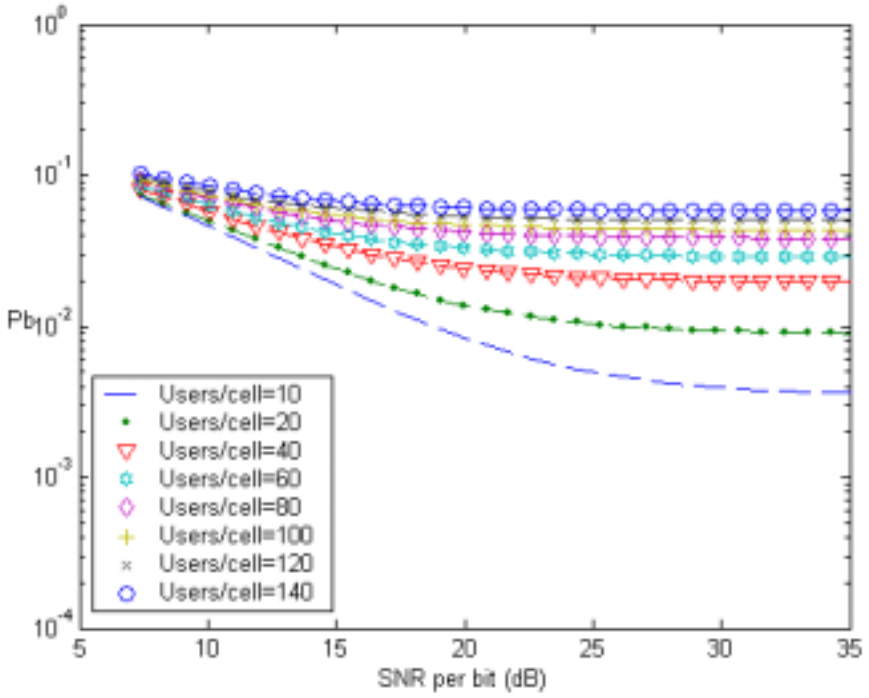

Figure 29. Performance for the DS-CDMA System with a Four-Element UCA ($\sigma_{\text{dB}} = 8$) for $N = 128$ in a Rayleigh Fading Channel

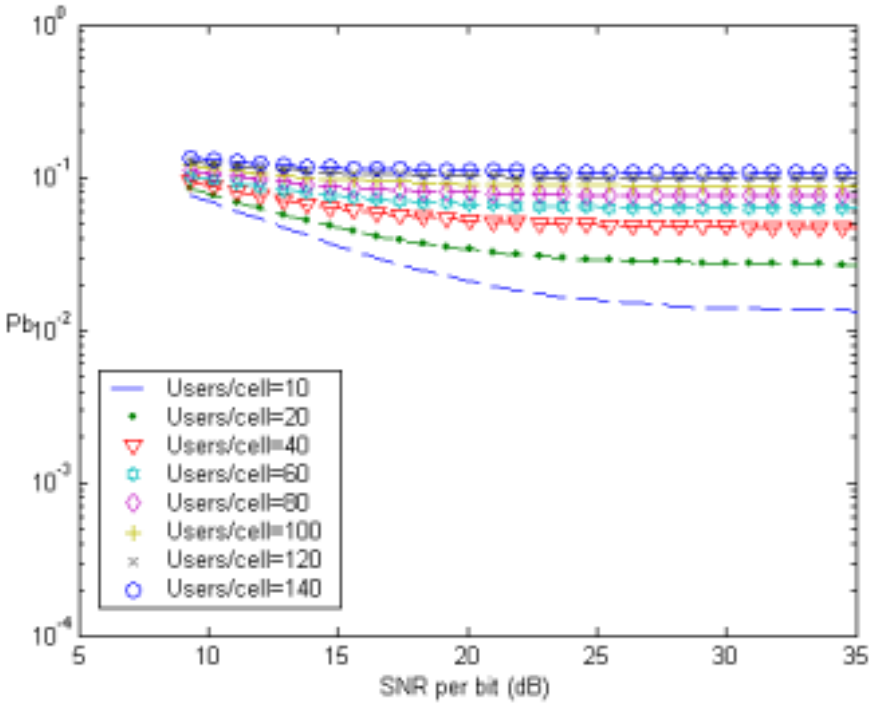

Figure 30. Performance for the DS-CDMA System with a Four-Element ULA ($\sigma_{dB} = 9$) for $N = 128$ in a Rayleigh Fading Channel

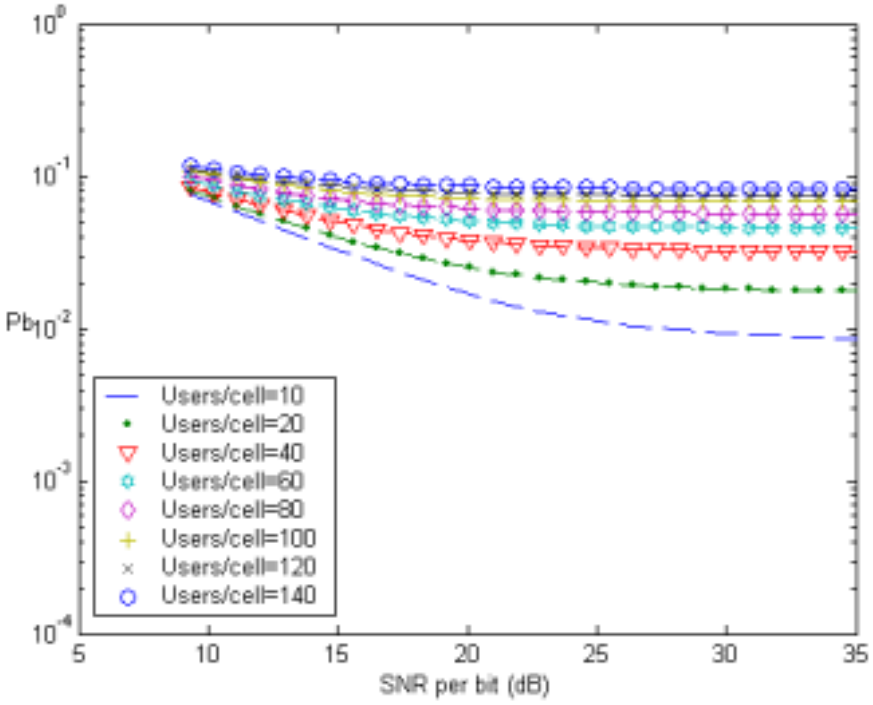

Figure 31. Performance for the DS-CDMA System with a Four-Element UCA ($\sigma_{dB} = 9$) for $N = 128$ in a Rayleigh Fading Channel

From these plots, it is evident that the DS-CDMA System with UCA outperforms its ULA counterpart in terms of BER performance. In addition, it had been demonstrated in Ref. [5] that the system's BER performance vastly improved when the DS-CDMA System was explored employing ULA. As such, the ULA is used as a baseline for the performance analysis in this thesis.

C. NAKAGAMI-M LOG-NORMAL CHANNEL FADING MODEL

As described earlier, fading observed in wireless communication channels is mainly due to multi-path. Although it is accurately modeled by the Rayleigh fading effect for short-distance and high frequency communications, the Rayleigh fading falls short in describing long-distance fading effects with sufficient accuracy [9]. This fact was first observed by Nakagami who formulated a parametric gamma distribution-based density function to describe the experimental data he obtained. Many researchers then showed that by using real-life data that Nakagami's proposed model provides a better explanation to both the less and more severe conditions than the Rayleigh model and better fits the mobile communication channel data [10].

In this thesis, we present simulations of the fading channels using a Nakagami-m fading with $m = 3$ and $m = 5$ respectively, as developed in Ref. [8]. This is an important issue as fading is inherently introduced in wireless communication channels. Furthermore, Nakagami model for fading is a general formulation that encompasses other important models like Rayleigh and Rician.

The plots in Figures 32 to 37 show the simulation results and the comparison of UCA that includes the average SNR per bit for a different number of active mobile users. For a given level of BER and a number of active users, the corresponding average SNR per bit can be determined for each configuration, namely:

a) $\sigma_{\text{dB}} = 7$, 8 and 9; for a four- element UCA and $m = 3$

b) $\sigma_{\text{dB}} = 7$, 8 and 9; for a four- element UCA and $m = 5$

Figures 32 and 33 illustrate the performance for the DS-CDMA System with a four-element UCA with $\sigma_{\text{dB}} = 7$ for a Nakagami-m log-normal channel with $m = 3$ and $m = 5$, respectively. It was observed that BER improves with a larger value of m that symbolized a little or no fading situation. For example, at $P_b = 10^{-4}$ and 20 users per cell, when $m = 3$, UCA requires a SNR per bit of 16 dB as compared to UCA that that is operating with $m = 5$ that requires only a SNR per bit of 10 dB.

Figures 34 and 35 illustrate the performance for the DS-CDMA System with a four-element UCA with $\sigma_{\text{dB}} = 8$ for a Nakagami-m log-normal channel with $m = 3$ and $m = 5$, respectively. As σ_{dB} is increased to 8, this corresponds to the system operating in a more severe fading environment and thus reduces the effectiveness of the adaptive antenna.

Figure 36 and 37 further reveal the performance for the DS-CDMA System with a four-element ULA and UCA, respectively, with $\sigma_{\text{dB}} = 9$ for a Nakagami-m log-normal Channel with $m = 3$ and $m = 5$, respectively. Clearly, the performance of the system is degraded under a hasher fading environment.

The slope of the P_b-SNR curve flattens out as illustrated in the plots. This means it requires a larger increase in SNR to achieve a certain amount of improvement in performance, whereas in the no-fading case, the same amount of performance can be achieved with a much smaller increase in SNR. The final observation was that as m gets smaller, the degradation in the performance increased as smaller m values were used.

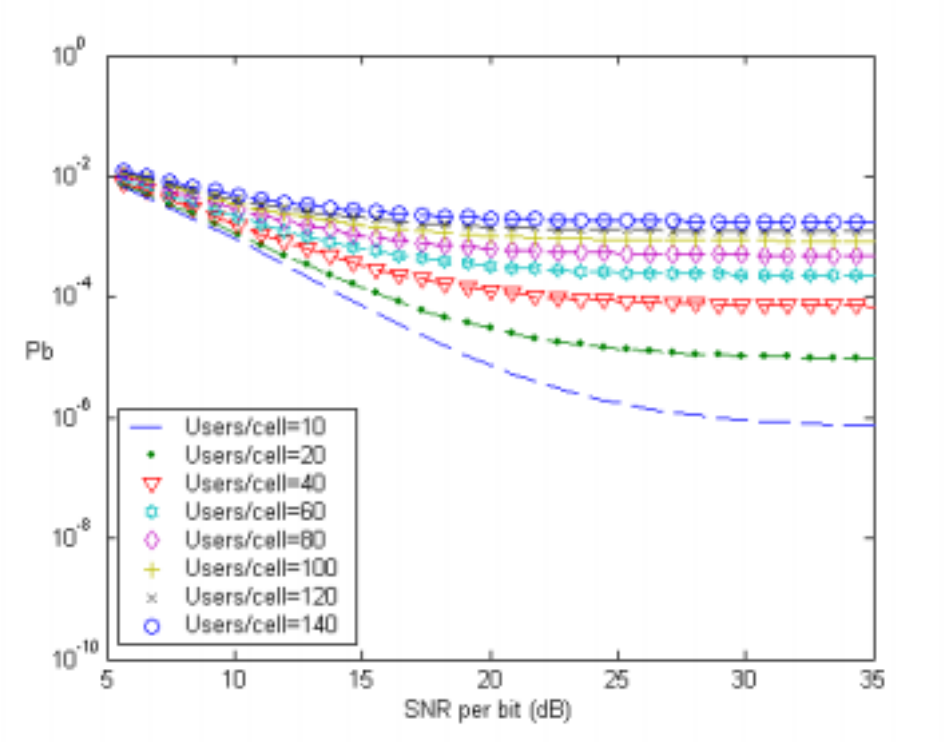

Figure 32. Performance for the DS-CDMA System with a Four-Element UCA ($\sigma_{dB} = 7$) for a Nakagami-m Log-normal Channel Fading Model with $m = 3$

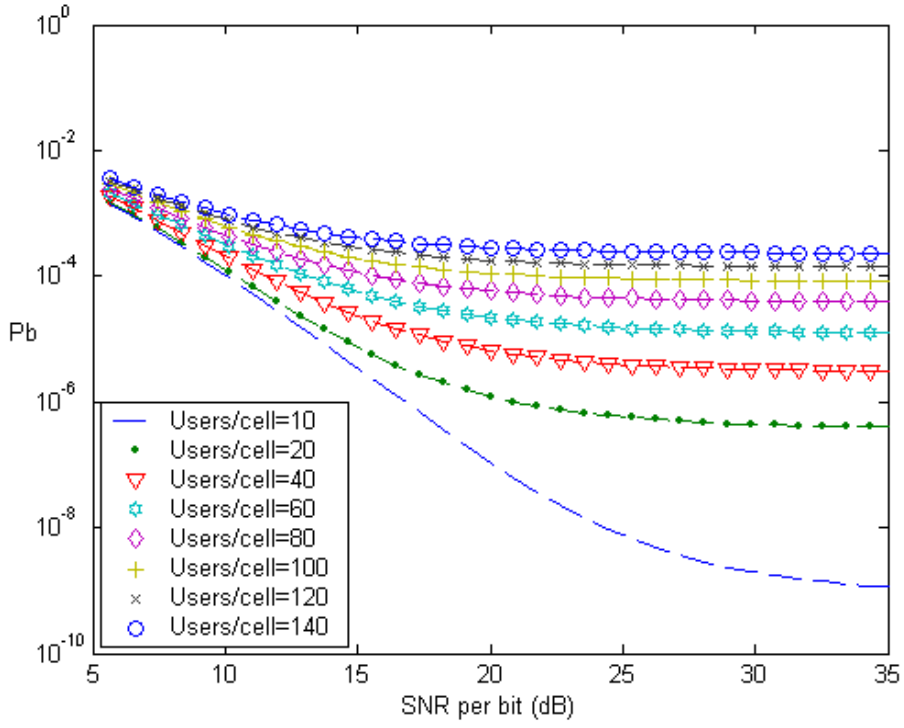

Figure 33. Performance for the DS-CDMA System with a Four-Element UCA ($\sigma_{dB} = 7$) for a Nakagami-m Log-normal Channel Fading Model with $m = 5$

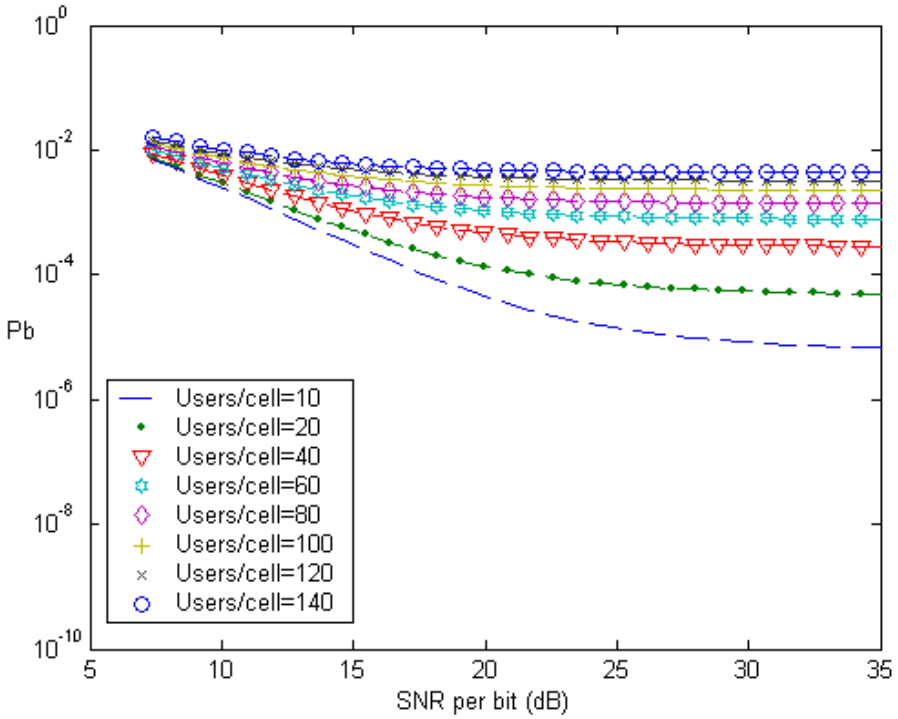

Figure 34. Performance for the DS-CDMA System with a Four-Element UCA ($\sigma_{dB} = 8$) for a Nakagami-m Log-normal Channel Fading Model with $m = 3$

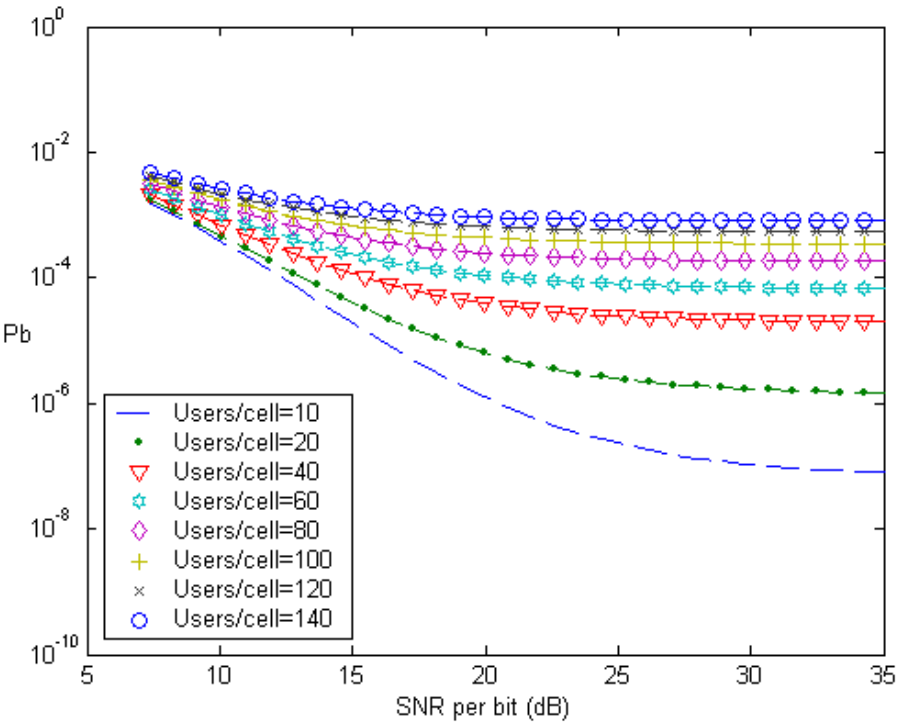

Figure 35. Performance for the DS-CDMA System with a Four-Element UCA ($\sigma_{dB} = 8$) for a Nakagami-m Log-normal Channel Fading Model with $m = 5$

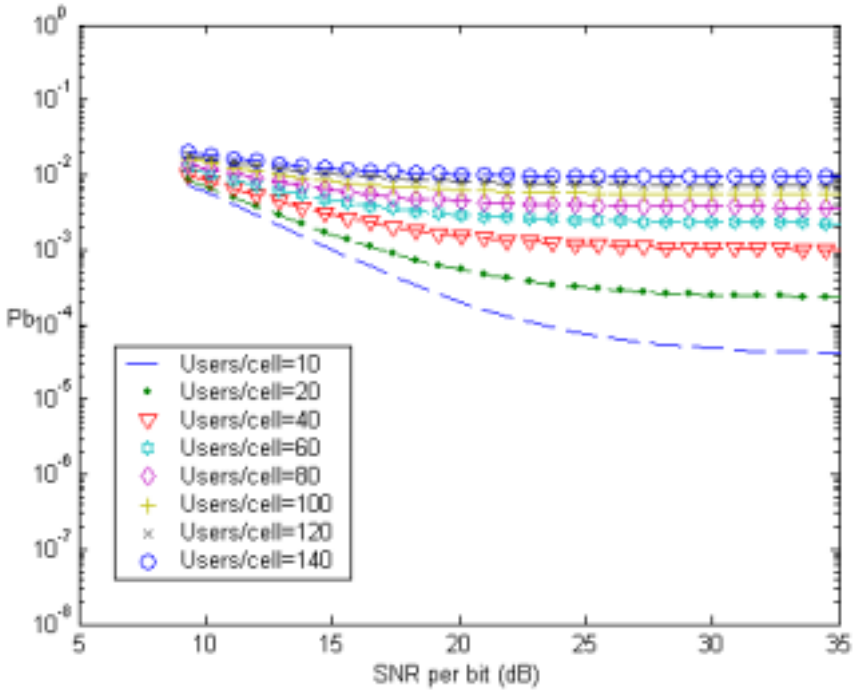

Figure 36. Performance for the DS-CDMA System with a Four-Element UCA ($\sigma_{dB} = 9$) for a Nakagami-m Log-normal Channel Fading Model with $m = 3$

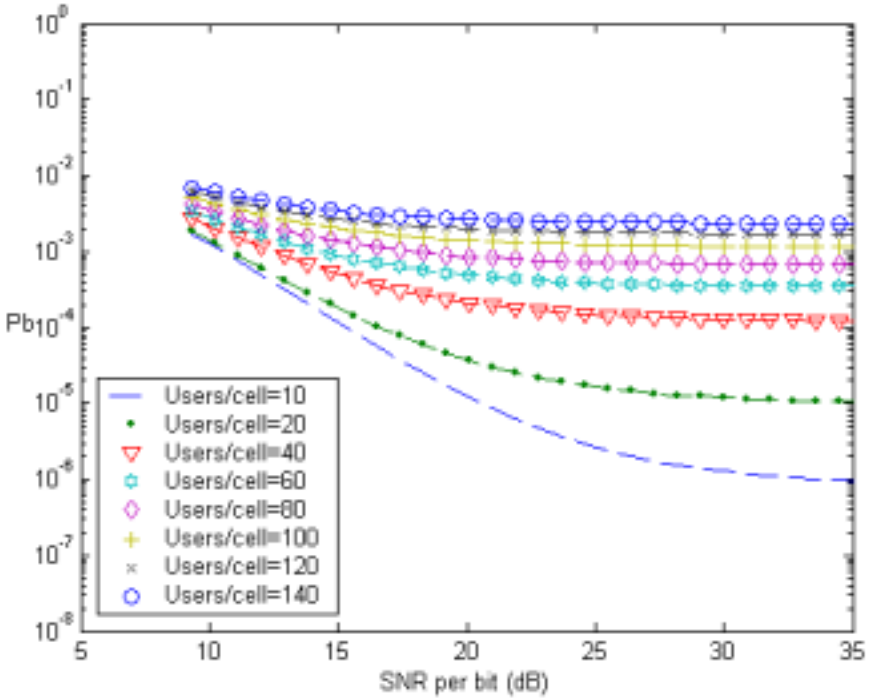

Figure 37. Performance for the DS-CDMA System with a Four-Element UCA ($\sigma_{dB} = 9$) for a Nakagami-m Log-normal Channel Fading Model with $m = 5$

D. ADVANTAGES OF UCA OVER ULA

1. 360° Field of View and Symmetry

The interest in uniform circular antenna arrays has been significant because of their 360^0 field of view and their numerous applications in military early warning and support systems, cellular networks, and surveillance. The UCA of a mobile communication system is an attractive alternative to the ULA mainly because of its 360^0 field of view. The performance of the UCA with a 360^0 field of view is superior to that of a ULA with only a 180^0 field of view. This fact leads to the symmetry problem inherent with ULA. For example, Figure 38 shows that the ULA antenna pattern is always symmetrical on two sides from an axis of about 90^0 to 270^0. If the DoA of the desired signal and the interferer fall on the opposite side, both the antenna factor and gain will be the same for the desired signal and the interferer. In a worst-case situation in which the interferers are located in this symmetrical location and if the interferers are equal distance or equal signal power to the mobile as the SBS signal, the ISR will be close to zero and that is not advantageous. Although the occurrence of this situation may be rare, it cannot be ruled out since the possibility of the mobile location cannot be pre-determined.

On the other hand, this situation can be overcome using an UCA due to its outstanding geometrical characteristics. Figure 39 demonstrates an identical situation in which the three- element UCA can overcome this limitation by virtue of its exceptional geometry characteristics. The computed ISR is –18.8 dB when one of the interfering signals is directly opposite the desired signal.

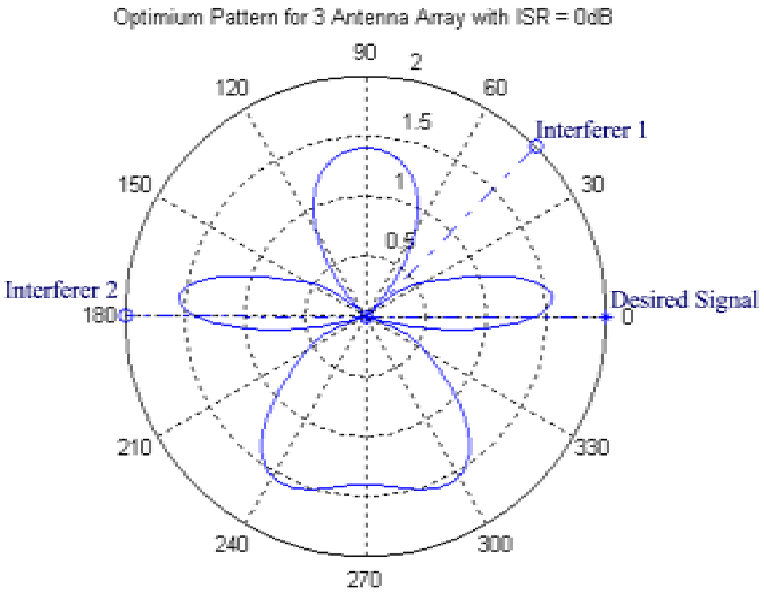

Figure 38. A Three-Element ULA with an Interfering Signal Directly Opposite the Desired Signal (From Ref. [5].)

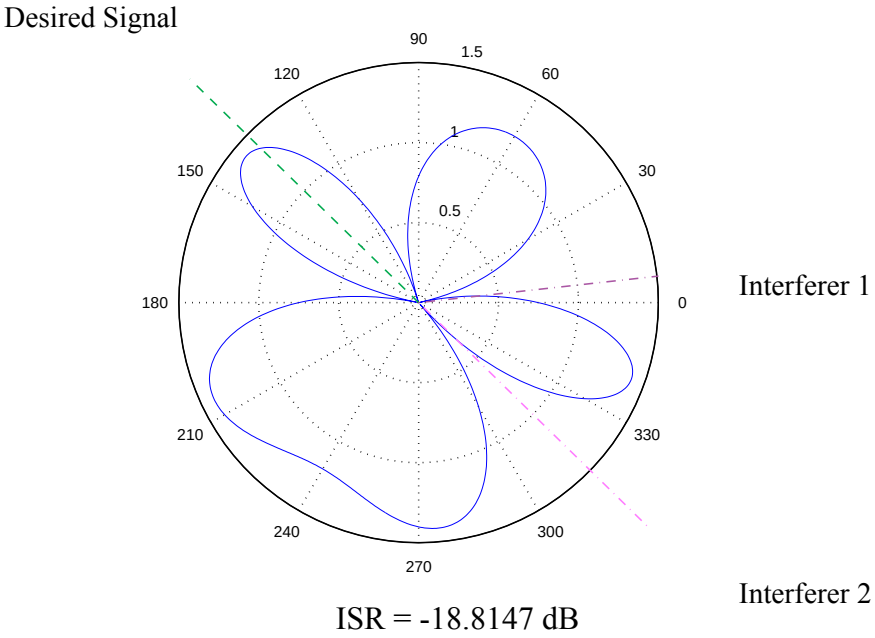

Figure 39. A Three-Element UCA with an Interfering Signal Directly Opposite the Desired Signal

2. Antenna Separation

If the angular spread between the desired signal and the interferer is small, the antenna array may not be able to discriminate the interferer signal with deep nulls unless the antenna separation is increased [5]. Figure 40 shows the pattern of a three-element ULA and antenna separation of $d = \lambda/2$. If the desired signal DoA is at 0^0 azimuth and two interfering signals with DoA is at 125^0 and 360^0 in azimuth respectively, the ULA can achieve an ISR of –7.12 dB. Subsequently, when the antenna separation for the ULA system is increased to $d = \lambda$, the ISR will improve from –7.12 dB to –127.84 dB, as shown in Figure 41. In general, the antenna array can provide a better interference cancellation if the antenna separation is increased, which is especially important when the angular spread of the different sources is small.

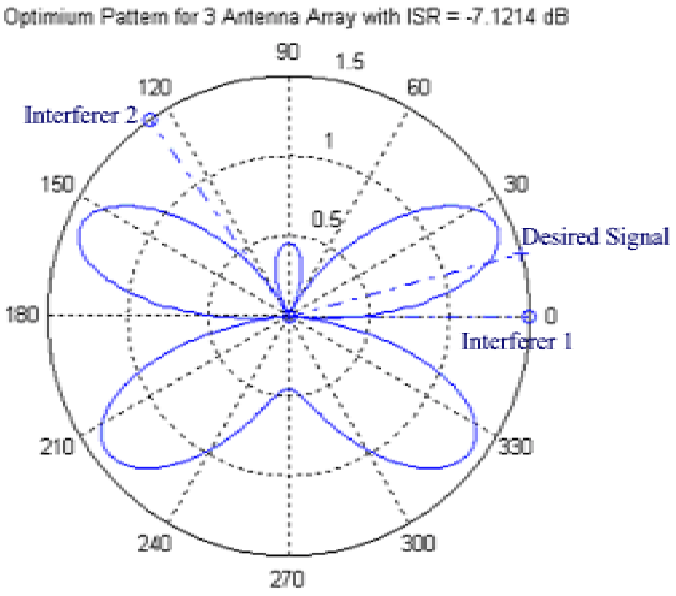

Figure 40. A Three-Element Linear Array Antenna Factor with ISR = –7.12 dB and $d = \lambda/2$ (From Ref. [5].)

However, for a mobile user, increasing the antenna separation is impossible in practice because of the very limited real estate for the antenna site. For a mobile terminal, such as a laptop PC, one can only fit up to a four-element linear array in about 45 cm, the

width of a typical laptop, with a antenna separation of $d = \lambda/2$ when operating in the frequency spectrum of 2 GHz. This is impossible if the antenna separation is increased to $d = \lambda$, which requires a width of more than 45 cm in practice.

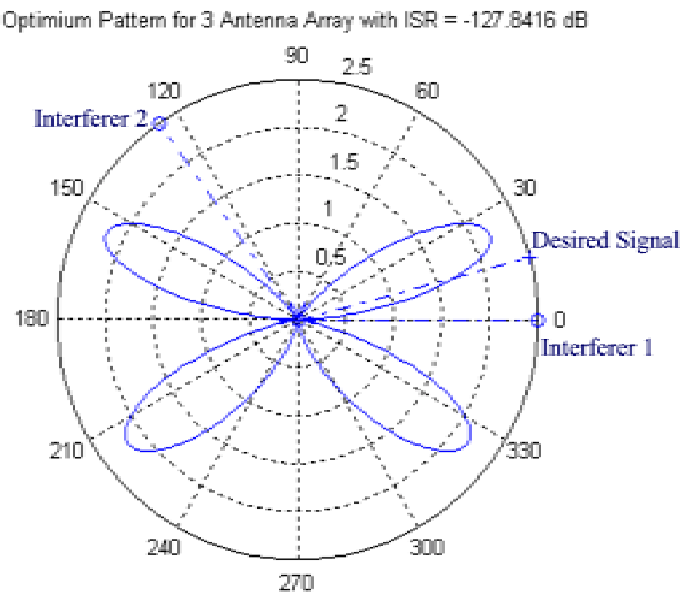

Figure 41. A Three-Element Linear Array Antenna Factor with ISR = –127.84 dB and $d = \lambda$ (From Ref. [5].)

Conversely, a four- or more elements UCA arranged in a circular pattern only requires a circular space with a radius of 15 cm. Hence, it is possible to fit an UCA with more elements on the mobile stations because the space required is constant as shown in Figure 42.

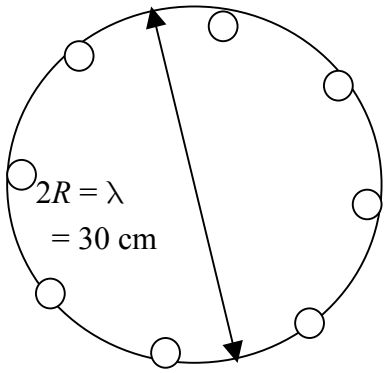

Figure 42. 8-element UCA

In general, an antenna array with more elements can nullify more interfering signals, thereby improving the system's performance and capacity significantly.

3. UCA in Space-Time Adaptive Processing Application

Space-Time Adaptive Processing (STAP) is an adaptive space-time processor. In the radar system, STAP are used to detect the presence and pinpoint the location of a small, maneuverable target under ground and airborne clutter, strong interference, and random receiver noise [6]. The output of the STAP algorithm is a weighted sum of the received signal. In general, the STAP weights are designed to enhance the desired signal and to reject interferences and noise. STAP has been applied in radar systems with ULA; however, the array orientation of the ULA limits the STAP in calculating the location of the target [6]. As such, the ULA can only provide the azimuth angle direction of the target.

Conversely, applying the UCA can provide the necessary information to estimate the elevation angle in addition to the azimuth angle direction of the target [6].

This Chapter illustrated the performance analysis of an adaptive antenna system in a circular pattern. Clearly, with the application of the smart antenna, the SINR of the system could be maximized. The next Chapter will discuss the performance analysis of wideband adaptive antenna system using a tapped-delay line.

THIS PAGE INTENTIONALLY LEFT BLANK

VI PERFORMANCE ANALYSIS OF WIDEBAND ADAPTIVE ANTENNA SYSTEM USING TAPPED-DELAY LINE

In the previous Chapters, the analyses assumed that the DS-CDMA system is a narrowband system in which a single complex circular adaptive weight in each element channel of a circular adaptive array properly processes narrowband signals. However, in order to process broadband signals, a tapped-delay line (transveral filter) is required. This tapped-delay line was employed because it could adjust the frequency dependent amplitude and phase.

In a practical implementation, each channel is slightly different electrically and will lead to channel mismatching, which could significantly alter the frequency response characteristics from channel to channel. This mismatch could cause significant differences in frequency response characteristics from channel to channel and may severely degrade the array performance [11]. Figure 43 shows the block diagram of the K-element antenna with L-tapped-delay line system. The multi-channel wideband processor consists of K sensors element channels in which, each channel contains one tapped delay line consisting of L tap points, (L-1) time delays of Δ seconds each, and L complex weights. The signals appearing at the second tap point in all channels are merely a time-delayed version of the signals appearing at the first tap point.

The tapped-delay line permits frequency dependent amplitude and phase adjustments to be made to equalize the frequency varying effect on the antenna when receiving a broadband signal. The weights in the tapped-delay line are chosen to maximize the signal-to-noise ratio (SNR), which is defined in Chapter V. As such, the performance of a system could be improved when multiple antennas are employed at the receiver. These signals at the antennas are sufficiently de-correlated with the use of diversity arrays, thus reducing signal interference.

Whether designing a tapped-delay line processor to accommodate broadband signals or to compensate for channel mismatch effects as described above, determining the number of taps that will be required to achieve a desired level of compensation is necessary. This is true because each additional tap and associated weighting element incorpo-

rated into the design increases the cost and complexity of the resulting adaptive array system. As such, the major question of how many taps are required for a specified set of conditions is an important aspect of practical design considerations.

This Chapter will analyze the performance of a DS-CDMA cellular system with a mobile terminal equipped with a adaptive array and a tapped-delay line by demonstrating the spectrum of the delay line transfer functions over a 4% bandwidth spread. The analysis further examines the effectiveness of various numbers of taps, namely for two, three and five taps, respectively.

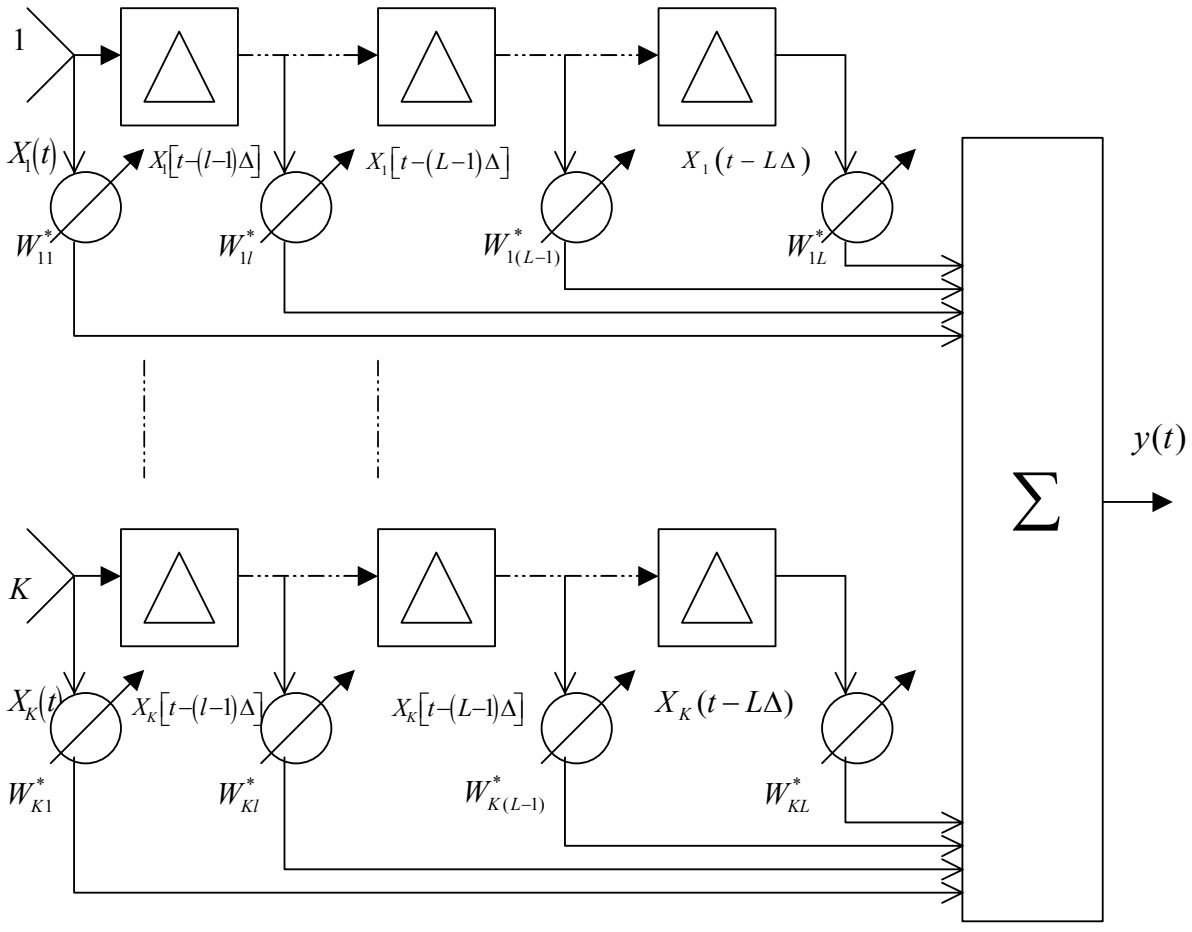

Figure 43. Wideband *K*-Element Array with an *L*-Tapped-Delay Line

The output of array, $y(t)$, is defined as:

$$y(t) = \sum_{l=1}^{L} \sum_{k=1}^{K} w_{kl}^{*} x_k \left[t - (l-1)\Delta \right] = W^{*} X(t), \tag{6.1}$$

where

$$W = \begin{bmatrix} W^{(1)} \\ W^{(2)} \\ . \\ . \\ W^{(L)} \end{bmatrix}, \quad W^{(1)} = \begin{bmatrix} w_{11} \\ . \\ . \\ . \\ w_{K1} \end{bmatrix}, \quad .... \quad W^{(L)} = \begin{bmatrix} w_{1L} \\ . \\ . \\ . \\ w_{KL} \end{bmatrix},$$

$$X(t) = \begin{bmatrix} X^{(1)}(t) \\ X^{(2)}(t) \\ . \\ . \\ X^{(L)}(t) \end{bmatrix}, \; X^{(1)}(t) = \begin{bmatrix} x_1(t) \\ . \\ . \\ . \\ x_K(t) \end{bmatrix}, \; X^{(2)}(t) = \begin{bmatrix} x_1(t-\Delta) \\ . \\ . \\ . \\ x_K(t-\Delta) \end{bmatrix}, \; . \; . \; X^{(L)}(t) = \begin{bmatrix} x_1\left[t-(L-1)\Delta\right] \\ . \\ . \\ x_K\left[t-(L-1)\Delta\right] \end{bmatrix}.$$

The transfer function $H(f)$ can be defined by taking the Fourier transform of the above $y(t)$,

$$H(f) = \frac{Y(f)}{X(f)} = \sum_{l=1}^{L} \sum_{k=1}^{K} w_{kl}^{*} e^{i2\pi f[(k-1)\tau + (l-1)\Delta]}, \tag{6.2}$$

where

$$\tau = \frac{d \sin\theta}{v}$$

The value of Δ is the inter-tap delay spacing (analysis using two, three and five tapped-delay line, $\Delta = \lambda_0 / 4$), v is the speed of light and d is the antenna array separation, and θ is the direction of arrival of the signal (either desired or interference).

It was observed that an array system with a tapped-delay line may be able to equalize the broadband signal, but only with a very complex algorithm and more computational power to determine an optimized set of weights [12]. In the case of a three-element array obtaining 6 weight values is required whereas a three element, three

tapped-delay line system requires 18 weight values. Clearly, the amount of time to determine a set of optimized weights increases significantly with the number of taps, which is critical for implementation. Hence the number of taps for a tapped-delay line implementation should be minimized to safeguard computation and evaluation time.

The tapped-delay line (transversal filter) processing is applied to each antenna element channel to allow frequency-dependent amplitude and phase adjustments for the broadband signals. The use of a tapped-delay line thereby provides the capability of equalizing the frequency varying effect on the antenna array when the latter is receiving a broadband signal.

The optimization was performed using MathCAD by minimizing the ISR at the center nominal frequency of the signals. The angle-of-arrival for the desired (SBS) signal and interference were assumed to be known and were used to determine the optimized complex weight values for the tapped-delay line. Figures 44, 45 and 46 show the optimized transfer functions *H(f)* in (Equation 6.2) of a three-element linear array with a two, three and five tapped-delay line at 4% bandwidth of the nominal center frequency respectively. It was observed that the optimized desired signal base-station (SBS) remains flat over the 4% bandwidth width while the transfer functions of the interference base-station (IBS) may fluctuate significantly over the same bandwidth. Although at the nominal center frequency, achieving excellent ISR suppression greater than –80 dB is possible, at the lower 4% band-edge the ISR suppression can only achieve a minimum of approximately –25 dB of ISR.

The three tapped-delay line response is presented in Figure 45. The most significant difference is that the interference signal response is reduced considerably, generally with a minimum rejection of the interference signal of more than 30 dB.

The five tapped-delay line response of Figure 46 is very similar to the three tapped-delay line response. The most significant difference is that it can achieve a better interference signal rejection of about 15 dB.

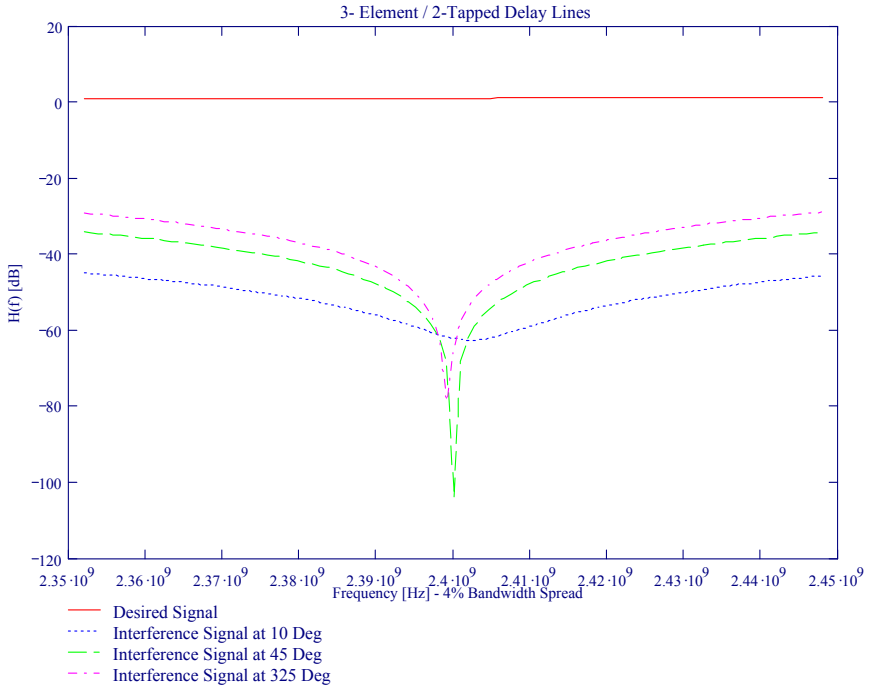

Figure 44. Desired Signal (SBS) and Interference Signal (IBS) Transfer Functions of a Three Element Array with a Two Tapped-Delay Line System and 4% Bandwidth

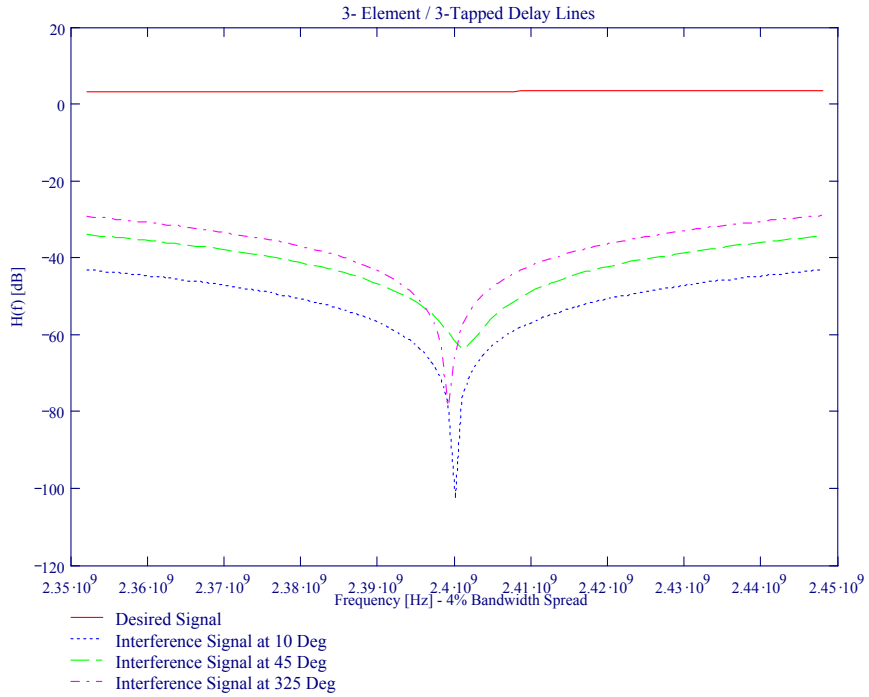

Figure 45. Desired Signal (SBS) and Interference Signal (IBS) Transfer Functions of a Three Element Array with a Three Tapped-Delay Line System and 4% Bandwidth

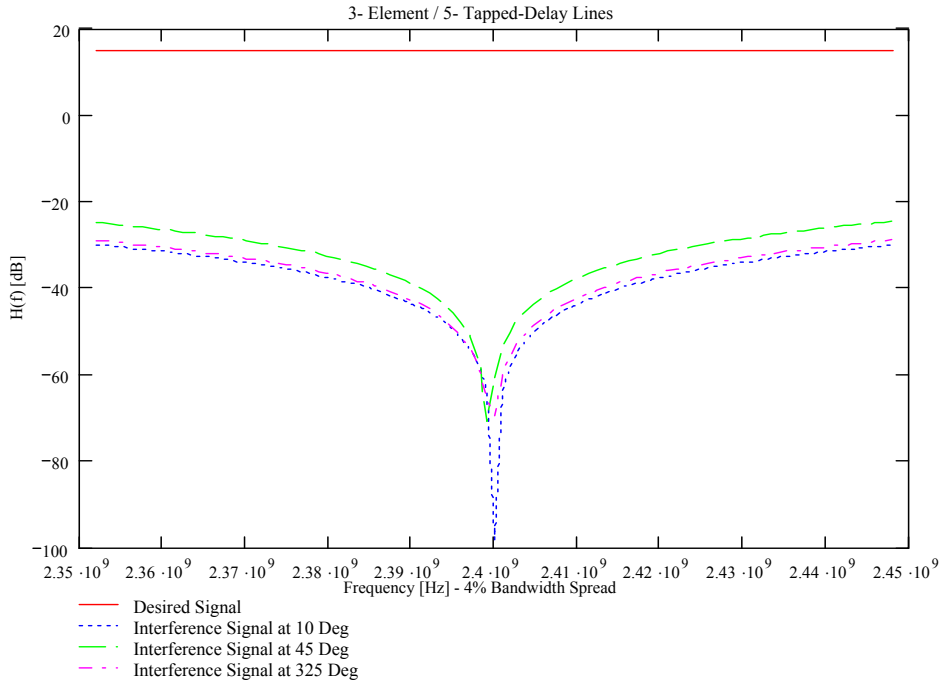

Figure 46. Desired Signal (SBS) and Interference Signal (IBS) Transfer Functions of a Three Element Array with a Five Tapped-Delay Line System and 4% Bandwidth

The entire process was repeated to obtain the optimum transfer functions for the four-element array system with two, three and five tapped-delay line, respectively, as shown in Figures 47, 48 and 49 on the next page.

It was observed that the optimized desired signal base station (SBS) transfer function, remains flat over the 4% bandwidth width while the transfer functions of the interference base station (IBS) may fluctuate significantly over the same bandwidth. Not only at the nominal center frequency is it possible to achieve excellent ISR suppression greater than –90 dB, but it can also achieve a minimum of about –30 dB of ISR at the lower 4% band-edge.

The three tapped-delay line response, presented in Figure 48, is very similar to the two tapped-delay line that is presented in Figure 47.

The five tapped-delay line response of Figure 49 is analogous to the three tapped-delay line response. The most significant difference is that it can achieve a better interference signal rejection of about 5 dB.

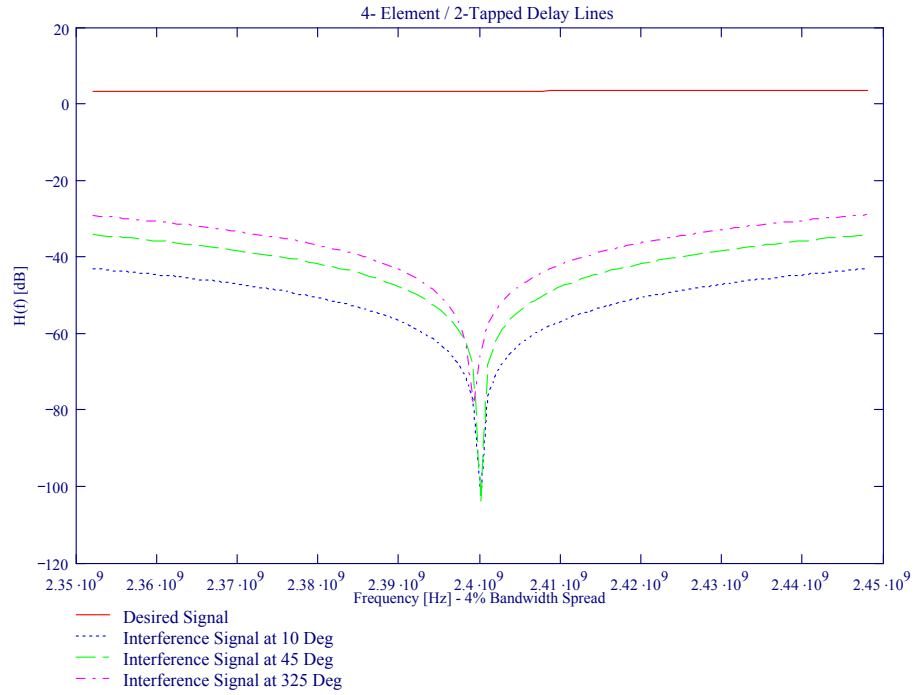

Figure 47. Desired Signal (SBS) and Interference Signal (IBS) Transfer Functions of a Four Element Array with a Two Tapped-Delay Line System and 4% Bandwidth

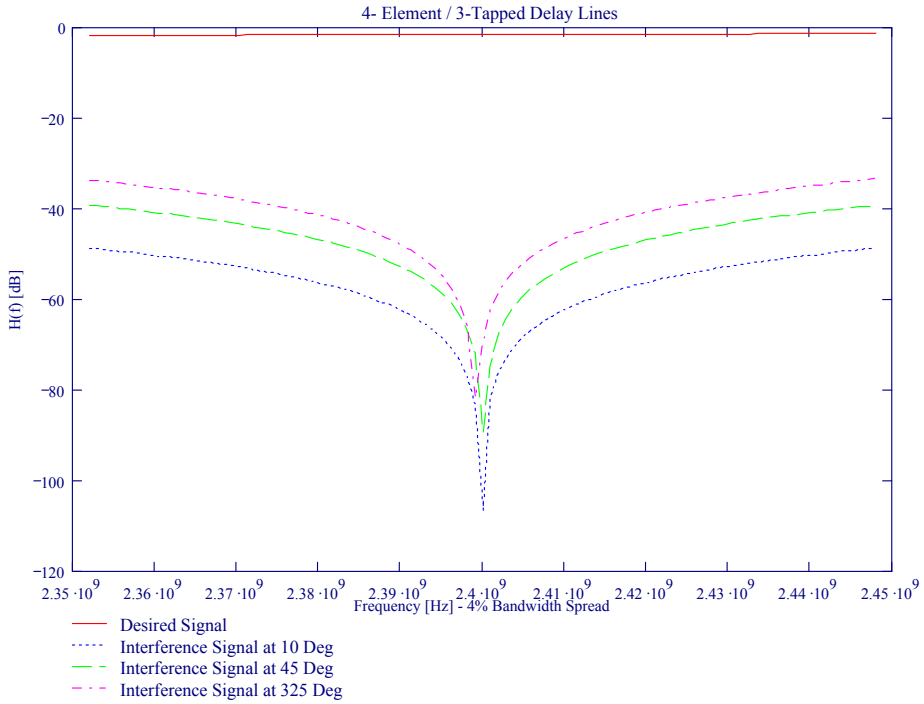

Figure 48. Desired Signal (SBS) and Interference Signal (IBS) Transfer Functions of a Four Element Array with a Three Tapped-Delay Line System and 4% Bandwidth

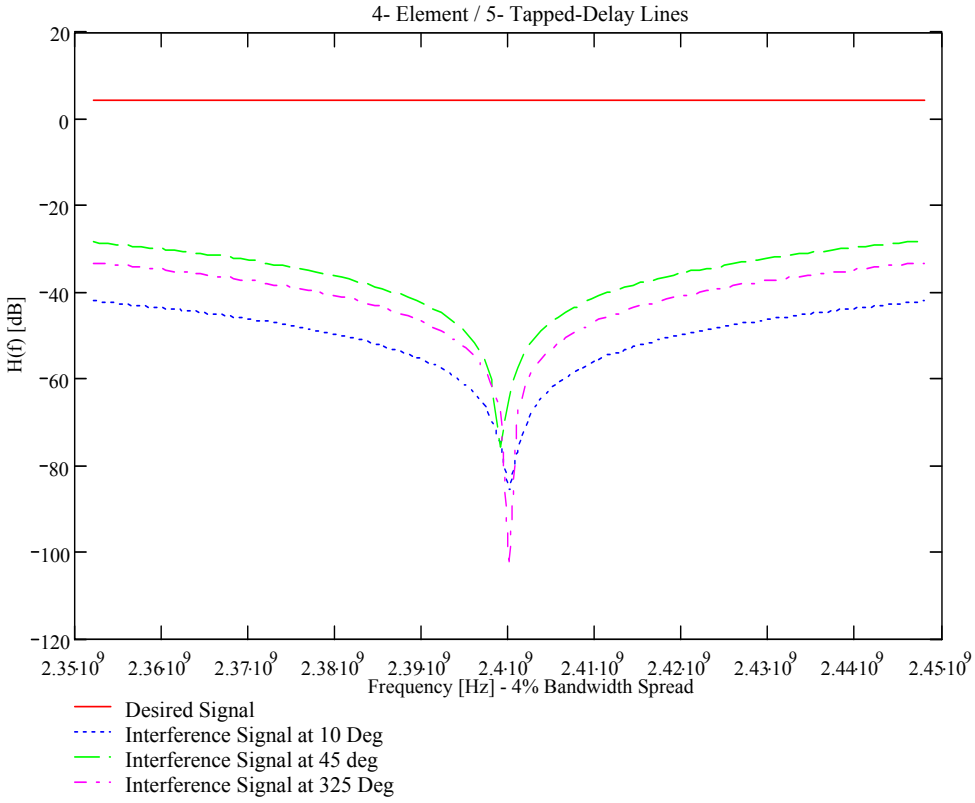

Figure 49. Desired Signal (SBS) and Interference Signal (IBS) Transfer Functions of a Four Element Array with a Five Tapped-Delay Line System and 4% Bandwidth

The ability of a tapped-delay line adaptive array to nullify interference depends strongly on the interference bandwidth. The optimal tap number of taps per array element may increase with a rise in fractional bandwidth. This is an important consideration factor especially with the move to wider bandwidths, such as in third-generation cellular networks that had also proposed the use of smart antennas in their deployment. This is a rapidly emerging application of antenna arrays and offers many advantages over space-only or time-only diversity.

In summary, the tapped-delay line consists of a sequence of weighted taps that offer a practical means for achieving the variable amplitude and phase weighting as a function of frequency. This is required for an adaptive array system to perform well against a

wideband interference signal sources. As such, a tapped-delay line provides an attractive means of compensating for the following system's undesirable effects:

a. Multi-path interference

b. Inter-channel mismatch

c. Propagation delay across the array

In this Chapter, the performance of a tapped-delay line application in a DS-CDMA mobile communication system was evaluated. The frequency varying effect of the broadband signal was equalized using a tapped-delay line. In general, for a four-element array system, two taps would be sufficient to equalize the broadband signal. However, for a three-element adaptive-array system, three taps may be required in order to give a better suppression at the center frequency. The next Chapter will conclude this thesis and proposes prospective developmental work in this arena.

THIS PAGE INTENTIONALLY LEFT BLANK

VII CONCLUSIONS AND FUTURE WORK

A. CONCLUSIONS

Undertaking this thesis project has provided the author with many learning opportunities regarding the smart antenna and its associated technologies. In particular, the author investigated the architectures with multiple antenna arrays arranged in a circular pattern that offered the advantages of higher gains, range extension, multi-path diversity, interference suppression, capacity increase and data rate increase. Smart antenna arrays have the ability to form a composite signal with higher performance, which increases the system's capacity by reducing interference from other users and increases the signal quality by reducing the fading effects. Adaptive antenna arrays can improve the performance of the received signal to a level that satisfies some pre-assigned criteria.

This thesis employed a uniform circular adaptive array at the mobile user terminal for a wideband DS-CDMA mobile communication system. A performance analysis was performed with a focus on the forward channel of the DS-CDMA system in a log-normal shadowing and Nakagami slow flat-fading environment. The application of the adaptive circular antenna array compounded the problem of obtaining a representative system performance boundary because the mobile terminal could be randomly located anywhere in the cell and the antenna array was orientation limited. Further, the performance of the array could also vary significantly with a small change in orientation.

The performance of the adaptive-array system for a broadband signal is also evaluated using a tapped-delay line. It has been demonstrated that the optimization process has been extremely computationally expensive and hence minimum taps should be used for practical consideration. The result obtained also illustrated that, in general, for a four-element circular array system, two taps would be sufficient to equalize the broadband signal while providing a performance level similar to that of a narrowband adaptive-array system.

The application of the adaptive array has allowed the DS-CDMA system to perform better because of the adaptive array's superior interference suppression and this allows the system to accommodate other constraining factors, such as higher fade depth.

The first generation FDMA/FM system (AMPS, TACS and NMT) use switched beam systems to improve the quality and capacity of the existing networks and to increase coverage in new markets. This is usually implemented on the forward link.

Second generation systems, both TDMA (IS-136 and GSM) and CDMA (IS-95) have had problems with smart antenna deployment. The air interfaces are such that smart antenna technology can be applied only under severe constraint. However, research is currently being conducted in this area and several trials are in progress on the mobile units.

Third generation mobile systems are based on Wideband CDMA or CDMA 2000. The W-CDMA air interface was designed to enable smart antenna deployment for increased capacity and coverage. This will enable the large-scale commercial deployment of adaptive antennas in mobile systems. Tapped-delay line structures are required because of the wideband nature of the signal and space-time processing can be implemented.

For further cellular "generations", incorporating the use of smart antenna technology into the design phase will be necessary. As these standards are still in the exploratory phase, it would be difficult to predict what aspects of antenna technology would be incorporated into their design. In addition, the continued use of smart antenna technology would depend on their impact in third generation systems, which have yet to be deployed.

Finally, smart antenna systems are attractive for mobile communications because they increase the carrier-to-interference ratio for users, which leads to higher capacity and lower network cost.

B. FUTURE WORK

1. Planar Adaptive Array

As a future research subject, the DS-CDMA system performance analysis with an adaptive array in a Rayleigh fading and Nakagami-m log-normal slow fading environment can be extended to a system using a planar adaptive array. This could be done in

"multiple dimensions" time and angle-of-arrival geometric model can also be incorporated into the system's performance analysis.

2. Jamming

In a military communication system, jamming is a serious threat. Jammers can affect the *ad hoc* network in two ways. Firstly, one or several nodes can be totally disconnected from the network. Secondly, one or several links may not be functional since the SINR becomes too low. This results in decreased capacity and increased average delays in the network. To be able to maintain communications in a military network having the ability to suppress these jammers is therefore important. Antenna arrays make this possible by minimizing the sensitivity in the direction of the jammer. Consequently, it would be interesting to study a scenario in which a jammer is present.

3. Smart Antenna in 3/4G Technologies

Fourth generation (4G) wireless technologies will provide data rates similar to office LANs or home cable modems and would be complementary to emerging 3G services. Smart antenna techniques, such as multiple-input multiple-output (MIMO) systems, can extend the capabilities of 3G and 4G systems to provide customers with increased data throughput for mobile high-speed data applications. MIMO systems use multiple antennas at both the transmitter and receiver to increase the capacity of the wireless channel. With these techniques, it may be possible to provide in excess of 1 Mbit/sec for the 3G wireless and as high as 20 Mbits/sec for 4G systems.

THIS PAGE INTENTIONALLY LEFT BLANK

LIST OF REFERENCES

[1] Janaswamy Ramakrishna, *Radiowave Propagation and Smart Antennas for Wireless Communications,* Kluwer Academic Publishers, Norwell, Massachusetts 2000.

[2] Theodore S. Rappaport, *Wireless Communications Principle and Practice*, 2nd Edition, Prentice Hall PTR, Upper Saddle River, New Jersey 2002.

[3] Tighe, J.E., "Modeling and Analysis of Cellular CDMA Forward Channel," PhD Dissertation, Naval Postgraduate School, Monterey, CA, March 2001.

[4] Theodore S. Rappaport and Joseph C. Liberti, JR., *Smart Antennas for Wireless Communications*, 1st Edition, Prentice Hall, Upper Saddle River, New Jersey 1999.

[5] Ng, Kok Keng, "Smart Antenna Application in DS-CDMA Mobile Communication System" MSEE Thesis, Naval Postgraduate School, Monterey, CA, September 2002.

[6] Michael, Zatman **"**Circular Array STAP" MIT Lincoln Laboratory, Seventh Annual ASAP '99 Workshop, New Jersey, March 1999.

[7] Tsai, Jiann-An and Woerner, Brian D, "Adaptive Beamforming of Uniform Circular Array (UCA) for Wireless CDMA System," presented at the 35th Asilomar Conference, California, November 2001.

[8] Ioannis, Karagiannis, "Development of a Nakagami-Lognormal Model for a Cellular CDMA Forward Channel" MSEE Thesis, Naval Postgraduate School, Monterey, CA, March 2002.

[9] Yip, K.W., T.S. Ng, "A Simulation Model for Nakagami-m Fading Channels, $m<1$," *IEEE Trans. on Comm*., vol. 48, no. 2, Feb 2000.

[10] Zhang, Q.T., "A Decomposition Technique for Efficient Generation of Correlated Nakagami Fading Channels," *IEEE Journal on Selected Areas in Comm*., vol. 18, no. 11, Nov 2000

[11] Monzingo, Robert A. and Miller, Thomas W, *Introduction to Adaptive Arrays,* John Wiley & Sons, Inc, New York, 1980.

[12] Hudson, J.E, *Adaptive Array Principles,* Institution of Electrical Engineers, London 1981.

INITIAL DISTRIBUTION LIST

1. Defense Technical Information Center
   Ft. Belvoir, Virginia

2. Dudley Knox Library
   Naval Postgraduate School
   Monterey, California

3. Chairman, Code EC
   Department of Electrical and Computing Engineering
   Naval Postgraduate School
   Monterey, California

4. Professor Tri T. Ha, Code EC/Ha
   Department of Electrical and Computing Engineering
   Naval Postgraduate School
   Monterey, California

5. Professor Jovan Lebaric, Code EC/Lb
   Department of Electrical and Computing Engineering
   Naval Postgraduate School
   Monterey, California

6. Major Stewart Siew Loon Ng
   Singapore